Chapter 2

Tbx20 function in autophagy in heart studied through *in-vitro* and *in-vivo* model systems.

Chapter 2

Tbx20 function in autophagy in heart studied through *in-vitro* and *in-vivo* model systems.

A. Introduction

Autophagy is an evolutionarily conserved catabolic phenomenon that recycles cellular components to provide for bioenergetics and fuel for cellular survival under stress conditions. At the basal level, the goal of the autophagic machinery is to maintain cellular and organ homeostasis. This is achieved by providing catabolites like fatty acids and amino acids which in turn serve as substrates for many metabolic processes and also by eliminating damaged organelles and misfolded proteins. The cargo (can be organelles, protein aggregates, lipids, cellular proteins) to be degraded is sent to lysosomes via autophagosomes whereby fusion of lysosomes with the latter forms autolysosomes and the cargo is thereafter degraded by lysosomal hydrolases. The catabolites released after degradation serves as substrates for cellular bioenergetics. Autophagy can also be activated under stress conditions like nutrient scarcity/ caloric restriction, ROS (Reactive Oxygen Species) accumulation, ER (Endoplasmic Reticulum) stress, and mitochondrial damage where autophagy serves as a substrate recycling machinery remove protein aggregates and provides much-needed ATP for the survival of cells.[9–11] In general, there are three different types of autophagy including microautophagy wherein the cargo to be removed is taken up directly by the invagination and protrusion of lysosomes and later destroyed by the lysosomal luminal hydrolytic enzymes. chaperone mediated autophagy in which chaperone HSPA/Hsc70 recognises proteins bearing the sequence tag KFERQ and then directs it to LAMP-2A (Lysosomal associated membrane protein 2A) for degradation and macroautophagy which involves the formation of double membrane sacs/vesicles occurs which engulfs the cytosolic constituents to be

removed. These double membrane structures then form autophagosome and eventually its fusion with lysosome leads to the formation of autolysosomes and the hydrolytic luminal enzymes lyse or degrade the cargo components.[95,96] Macroautophagy (also called autophagy) is a multi-step process including induction, nucleation, expansion of phagosome and fusion of lysosome to form autolysosome and it is the contributes to the major portion of autophagy among the three types.[95,96] Under or over regulated autophagy and thus impaired autophagic flux is quite detrimental to the cells and tissues as such and often leads to severe pathophysiological conditions.[18]

Autophagy has been known to be a critical factor in the survival of neonates postpartum wherein it was found that Atg5 knockout mice models failed to survive after birth. Furthermore, in mice that survived the brief period of nutrient deprivation postpartum (which is the usual scenario), massive upregulation of cardiac autophagy was observed giving away the importance of autophagy in pro-survival while also bringing cardiac autophagy to the centre.[12] Cardiovascular diseases are a leading cause of global mortality and a major health concern.[82,97] So are cardiac aging and senescence. Impaired and altered autophagy has been an underlying cause of cardiac diseases like acute myocardial infarction (AMI) , Ischemic heart disease (IHD) and cardiomyopathy. Autophagy plays a controversial role during reperfusion injury where excessive autophagy leads to autosis but offers a protective during Ischemia and compensates for the low energy levels and nutrient scarcity that prevail during ischemic conditions. A similar role of autophagy has been found in acute myocardial infarction (AMI) wherein inhibition of autophagy enlarges the infarct zone and decreases the ATP content of cardiomyocytes and there have been theories that augmenting autophagy would be a therapeutic approach in restoring the cellular integrity and cardiac functioning in these cases.[13–17]

Aging is one of the major risk factors for a number of diseases including but not limited to cardiovascular and neurodegenerative diseases.[98] Aging is commonly

associated with telomere shortening, epigenetic alterations and ill-performing autophagy machinery. Mutations in Atg genes are associated with rapid aging or decreased lifespan in *Caenorhabditis elegans* and *Drosophila melanogaster*. Aging is perhaps one of the greatest risk factors responsible for failing hearts. In fact, aged individuals with no underlying cardiac condition show poor cardiac functionality, diastolic function and left ventricular dilatation.[18–20] Accumulation of protein aggregates, misfolded proteins, a poor balance between ROS and anti-oxidants, mitochondrial derangements, attenuated expression of Sirtuins (a class of NAD^+ dependent class-III deacetylating enzymes) especially Sirtuin 1, 3 (Sirt 1,3), GSk-3β contribute to cardiac aging.[21–23] Sirt1 has been known to regulate aging via processes like apoptosis, stress response and metabolism. All seven Sirtuin mammalian orthologs including Sirt1 have been studied in an array of diseases including diabetes, neurodegenerative, metabolic and cardiovascular diseases. The expression of Sirt1 has also been implicated to improve under caloric restriction/ starvation conditions while its expression declines massively with age including its expression in heart.[22] As such, impaired and poor levels of autophagy and scare expression of Sirtuins especially Sirt1 and 3 are prevalent in aging hearts while also apoptotic levels are on a surge. Overexpressing Sirtuin1, augmenting autophagy by either calorific restriction or Rapamycin administration has shown improvement in cardiac functioning and improved life longevity.[24–26] Tbx20, a T-box transcription factor and member of Tbx1 subfamily, is known to be crucial for cardiogenesis and murine models with Tbx20 knockout fail to survive beyond E10.5 due to hypoplastic hearts.[99] Tbx20 mutations correspond with severe congenital heart defects including valvulogenesis and septal defects.[1–3,76] Tbx20 is a pre-requisite for heart looping and important for the proliferative capacity of developing cardiomyocytes. Additionally adult mice heterozygous germline null for Tbx20 show conduction defects. An important characteristic of T-box proteins is the presence of a DNA binding domain[84]. The T-box domain of Tbx20 consists of 180 amino acid residues and Tbx20 has a binding affinity to

T/2 site [(**5'**-…AGGTGTGA…-3' or 5'-…AGGTGTGA…-3', or 5'-…AGGTGNTGACAG…-3'over the consensus T-site 5'-…TCACACCT…-3'].[79] It is the dual role as both transcriptional activator and repressor of Tbx20 that regulates the structure and function of heart. Tbx20 promotes cardiomyocyte proliferation via the Bmp2/pSmad1/5/8 and PI3K/AKT/GSK3β/β-catenin signaling pathways.[100] Tbx20 has also been found to act as a cardio-protectant against oxidative stress and downregulation of Tbx20 has been linked to increased apoptosis in cultured rat cardiomyocytes.[101] Further, the cardio-protective role of Tbx20 under ROS and hypoxic conditions in the H9c2 cell line was reported.[6] Tbx20 is known to interact with and induce other transcription factors like Nkx2.5 and Gata4[8,102] which are also important for cardiogenesis suggesting a unifying transcriptional role of Tbx20 in maintaining cardiac homeostasis and promoting the expression of Troponin-I and myosin heavy chain protein.

Here in this study for the first time, we demonstrate the role of Tbx20 as a potential candidate to induce anti-senescence-like characteristics in the aging mice population. Autophagy induced expression of Tbx20 activates GSK-3β and transcription factors Nkx2.5, Gata4 and Sirt1 after subjection to starvation and rapamycin treatment in both in-vivo (BALB/c mice) and in-vitro (H9c2 cell line) model systems. The upregulation of Nkx2.5 and Gata4 following autophagy induction is indicative of progression towards progenitor like cardiomyocyte characteristics, while activation of Sirt1 and GSK3β suggests an anti-aging/ senescence since Sirtuin1 is closely linked with aging, is known to be a mediator of caloric restriction and Sirt1 transgenic mice prevent early mortality. Very interestingly, the promoter region of Sirt1 DNA from both *Rattus norvegicus* and *Mus musculus* was found to harbour the T/2 binding site- 5'-AGGTGTGA-3' within a conserved consensus sequence making Sirt1 a possible candidate to interact with Tbx20. To finally re-affirm our in-silico finding, Tbx20siRNA mediated knockdown was performed in H9c2 cells. The results following Tbx20

LOF assay in the H9c2 cell line confirmed Tbx20-dependent expression of Sirt1 along with GSK-3β and previously mentioned interactions of Tbx20 with both Nkx2.5 and Gata4.[102] The finding of a potential interaction between Tbx20 and Sirt1 is not only a novel revelation but also of clinical importance. It holds a therapeutic value as targeted delivery of Tbx20 in aging hearts could improve the stigmatised hallmarks of aging in heart and might improve cardiac functioning by Tbx20 mediated positive upregulation of Sirt1 in addition to the beneficiary effects brought by Tbx20 regulated expression of Gata4 and Nkx2.5 provided simultaneously autophagy flux is balanced.

B. Methods

Animal study and experimentation

All experiments and protocols involving animals were reviewed and approved by the Institutional Animal Ethics Committee of Presidency University, (PU/IAEC/SC/18). BALB/c male mice, aged 26-28 months were used for this study. Animals were either treated with starvation (Strv) where mice were starved for 48 hours (water was provided *ad libitum*) or treated with Rapamycin (Rap) (TC416, Himedia) administered intraperitoneally every alternate day for 8 weeks at a concentration of 4mg/kg to induce autophagy.[11,103,104] Control group was a similar age and sex matched. After completion of the experiment, whole hearts were then harvested and proceeded with for either Western Blot (WB) or Immunohistochemistry (IHC).

Immunohistochemistry.

Whole hearts were harvested, washed in 1X PBS and fixed in 4% paraformaldehyde, after which the tissue was dehydrated and embedded in paraffin. Tissue sections of size 5μm was cut using a microtome (Leica Biosystems). Later IHC was performed as previously described [105] having used Citrate buffer (pH-6) for antigen retrieval and the stained sections were mounted

in mounting media (20mM Tris, pH-8, 90% glycerol, 0.5% N-propyl gallate). Primary antibodies used were Tbx20 (2µg/ml, PA5-40669, Invitrogen) and Sirtuin-1 (1:1000, MA5-27216, Invitrogen,), mTORC1 (1:1000, ab109268, Abcam), GSK-3β (1:1000, 27C10, CST) and pGSK-3β (1:1000, ab131097, Abcam). The secondary antibodies used were either Alexa flour 488 goat anti-rabbit secondary antibody (ab150077, Abcam) or Alexa flour 594 goat anti-mouse secondary antibody (ab150116, Abcam) were added against their respective primary antibodies, both used at dilution 1:2000. DAPI (D9542, Sigma) used at a 1:400 dilution was used as a nuclear stain. Images were acquired using a Leica epi-fluorescence microscope and LasX software.

Cell Culture

The in-vitro studies were carried out on H9c2, a rat ventricular cardiomyoblast cell line. The cells were maintained in DMEM (AT007, Himedia) media supplemented with a 2% Penicillin-Streptomycin cocktail (A004, Himedia) and 10% FBS (RM10409, Himedia). The cells were maintained in a sterile humidified incubator with CO_2 maintained at 5% levels and 95% air. Cellular confluency of 75-80% was used for experimental purposes. For Starvation induction cells were washed 3X with 1XPBS, after which cells were incubated with serum and glucose-free DMEM (AT195, Himedia) for 5 hours.[106] For Rapamycin induced autophagic response cells were treated with 10nM Rapamycin (TC416, Himedia) for 1 hour.[24]

RNA isolation, RT-PCR, and real-time PCR

Total RNA was extracted using the Trizol-Chloroform technique from untreated and treated H9c2 cells. The Biorad cDNA synthesis kit was used to create cDNA from 1 µg of total RNA. (iScript™ Reverse Transcription Supermix for RT, 170-884) in 20 µl of total volume according to manufacturer's protocol. The cDNA prepared was used for primer optimization using DNA Taq polymerase (by RT-

PCR in reverse time for real-time PCR against primers (BIOTAQ DNA polymerase BIO-21040, Bioline,). The rodent primer pairs Tbx20, Lc3b, Gabarpl1, Beclin1, mTORC1, Sirt1 and β-actin were used for PCR and Real-time PCRs. The Bio-Rad real-time PCR kit (172-52 03AP, SSO quick Eva green super mix) was used to perform the real-time PCR. β-actin was used to normalise the gene expression .

siRNA mediated transfection

For Tbx20 knockdown, Tbx20 specific siRNA (50pMol) (Ambion) aided with Lipofectamine RNAiMax reagent (13778-075, Invitrogen) mediated transfection was performed in H9c2 cells at 70-75% confluency for 48 hours following manufacturer's protocol. Before transfection H9c2 cells were subjected to starvation and rapamycin treatment to induce autophagy.

Western Blotting

Protein isolation was done using ice-cold mammalian lysis buffer (250 mM NaCl, 50 mM Tris pH 7.5, 0.1% SDS, 1% TritonX, and 5 Mm EDTA) containing protease inhibitor Pefabloc SC (11429868001, Roche) and phosphatase inhibitor (GX-0211AR, Genetix). For tissue samples, homogenisation was performed followed by a snap chill. The proteins were stored in small aliquots at -80°C until further use for Western Blotting (WB). Western blotting was performed as previously described.[107] The immunoblots were developed using Clarity™ ECL Substrate (1705060, Bio-Rad) and scanned using ChemiDoc MP (BioRad). The primary antibodies used were anti-Tbx20 (2µg/ml) (PA5-4669, Invitrogen), anti-Lc3b (1:1000) (ab48394, Abcam), anti-GSK3β (1:1000, 27C10, CST), anti-pGSK-3β (1:1000, ab131097, Abcam), anti-Beclin1(1:1000, ab207612,Abcam), anti-Nkx2.5 (1:1000, PA5-85215, Invitrogen), anti-Gata4 (1:1000, ab227512 Abcam), anti-Sirtuin1(1:1000, GTX134606, Genetex). After overnight probing

at 4°C with these primary antibodies, the immunoblots were incubated with the corresponding HRP-tagged secondary antibodies, either a HRP conjugated secondary goat anti-rabbit (ab97051, Abcam) or a HRP conjugated goat anti-mouse secondary antibodies (ab97023, Abcam) were added against their respective primary antibodies at a dilution of 1:3000. The SDS gels were stained with 2.5% Coomassie (Brilliant blue G, SRL) and de-stained with coomassie de-stainer to obtain total protein intensities. The coomassie stained gels were scanned using ChemiDoc MP mentioned earlier. Quantification of intensities was done using ImageJ software (NIH).

Immunostaining

Immunostaining with H9c2 cells was performed as previously described.[108] The antibodies used were anti-Tbx20 (PA Invitrogen) used at a dilution of 1:500, anti-Beclin1 (1:1000, ab207612, Abcam),), anti-GSK3β (1:1000, 27C10, CST), anti-pGSK-3β (1:500, ab131097, Abcam), anti-Nkx2.5 (1:1000, PA5-85215, Invitrogen), anti-Gata4 (1:1000, ab227512, Abcam) and anti-Sirtuin1(1:1000, GTX134606, Genetex). The secondary antibodies used were either Alexa flour 488 goat anti-rabbit secondary antibody (ab150077, Abcam) or Alexa flour 594 goat anti-mouse secondary antibody (ab150116, Abcam) was added against their respective primary antibodies. DAPI (D9542, Sigma) used at a 1:400 dilution was used as a nuclear stain. Images were acquired with the help of Leica inverted epifluorescence microscope and LasX software. Later cell counting and fluorescence quantification was done with the help of ImageJ software (NIH).

Apoptosis/Necrosis detection assay

After subjecting H9c2 cells to starvation and rapamycin treatment, the cells were stained with either Cytocalcein violet 450 (CV450) following which live cell fluorescence imaging was recorded. In addition to CV450, the cells were stained with Apoxin Green (AG) and 7-Aminoactinomycin D (7-AAD) following the

manufacturer's protocol (ab176749, Abcam) and thereafter imaging was performed with Leica inverted epifluorescence microscope as mentioned earlier. H9c2 cells treated with Paclitaxel (ab, Abcam) at a concentration of 80nM for 12 hours were used as a positive control for the apoptosis experiment.[109]

In-silico assay:

Promoter Analysis of Sirtuin1- Sequences of Sirtuin 1 (Sirt1) of *Rattus norvegicus* and *Mus musculus* were obtained from NCBI[110] and screened for the presence of a consensus T-box binding sequence AGGTGTGA upstream of the coding region of Sirt1.

Statistical Analysis

Statistical analysis was performed with the help of GraphPad Prism 9.3.1 software. All the results are represented as mean ± Standard deviation of the mean (SD) or as median, quartiles and range. Statistical analyses were done using student's unpaired two-tailed T-test and one-way ANOVA for more than 2 groups. Differences among the groups were considered statistically significant for $P < 0.05$.

C. Results

Autophagy induced reactivation of Tbx20 in H9c2 cells and murine model.

The reactivated expression of Tbx20 along with the expression of Lc3b, Beclin1, gabarapl1, mTORC1 and Sirt1 was assessed with qPCR assay. (Fig. 1a, b, c, d, e and f) An enhanced expression of Lc3b and Gabrapl-1 for starvation and rapamycin treated cells confirmed successful autophagy induction following starvation and rapamycin treatment. mTORC1 was found to be inhibited following starvation and rapamycin treatment compared to the control group. Tbx20 and Sirt1 mRNA expression was found to be elevated for starvation and rapamycin treated groups respectively as compared to the control group. The

expression of Lc3b, Gabarapl1, Tbx20 and Sirt1 at mRNA levels was also assessed by qPCR *in-vivo* mice system. Mice treated with starvation and rapamycin showed similar upregulation in the levels of Lc3b and Gabrapl1 (Fig 1 g, h) confirming successful autophagy induction. The levels of Tbx20 and Sirt1 (Fig. 1 i, j) were also upregulated similar to the i*n-vitro* findings.

Figure 1

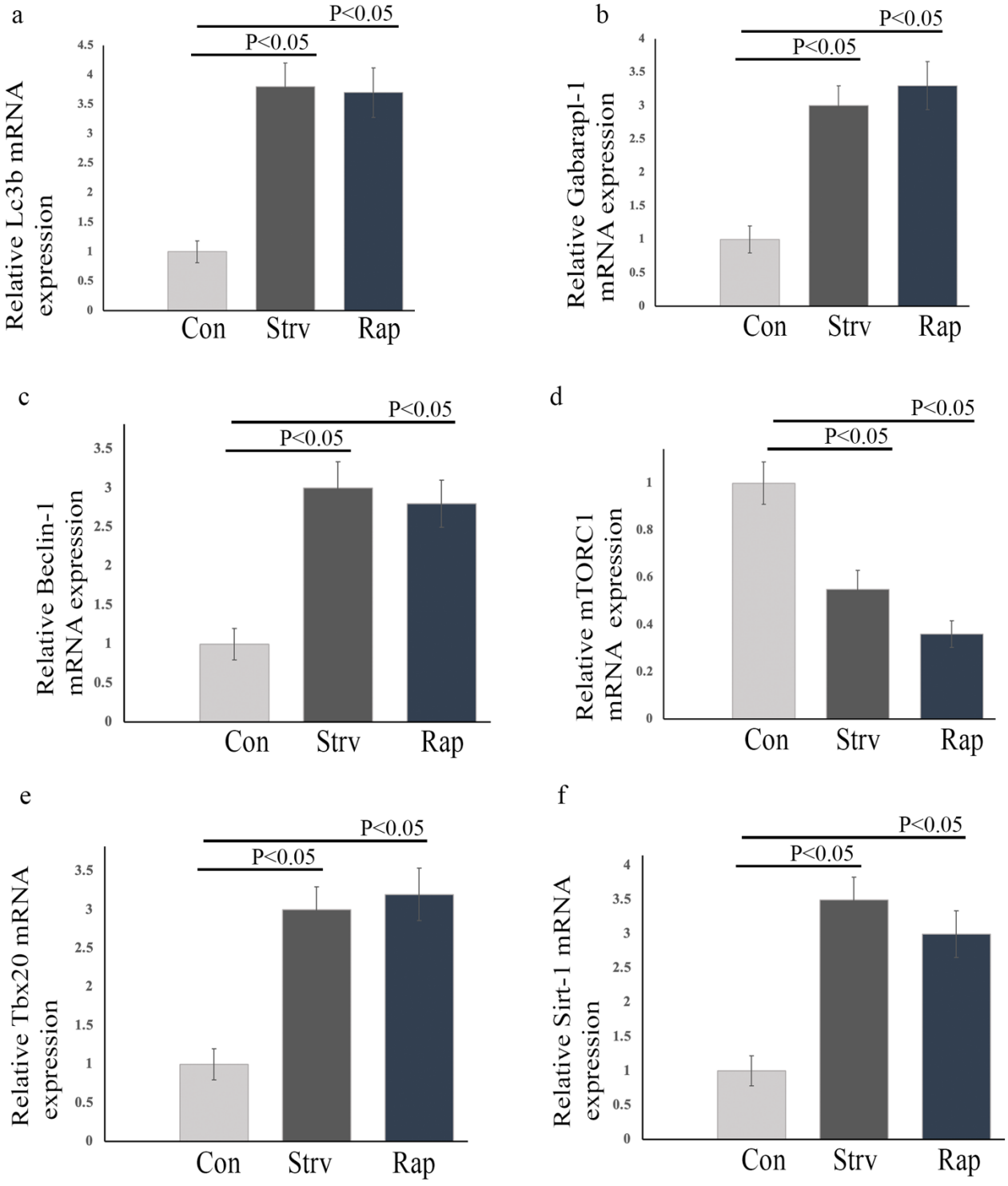
a
P<0.05
P<0.05
Relative Lc3b mRNA expression
Con
Strv
Rap
b
P<0.05
P<0.05
Relative Gabarapl-1 mRNA expression
Con
Strv
Rap
c
P<0.05
P<0.05
Relative Beclin-1 mRNA expression
Con
Strv
Rap
d
P<0.05
P<0.05
Relative mTORC1 mRNA expression
Con
Strv
Rap
e
P<0.05
P<0.05
Relative Tbx20 mRNA expression
Con
Strv
Rap
f
P<0.05
P<0.05
Relative Sirt-1 mRNA expression
Con
Strv
Rap

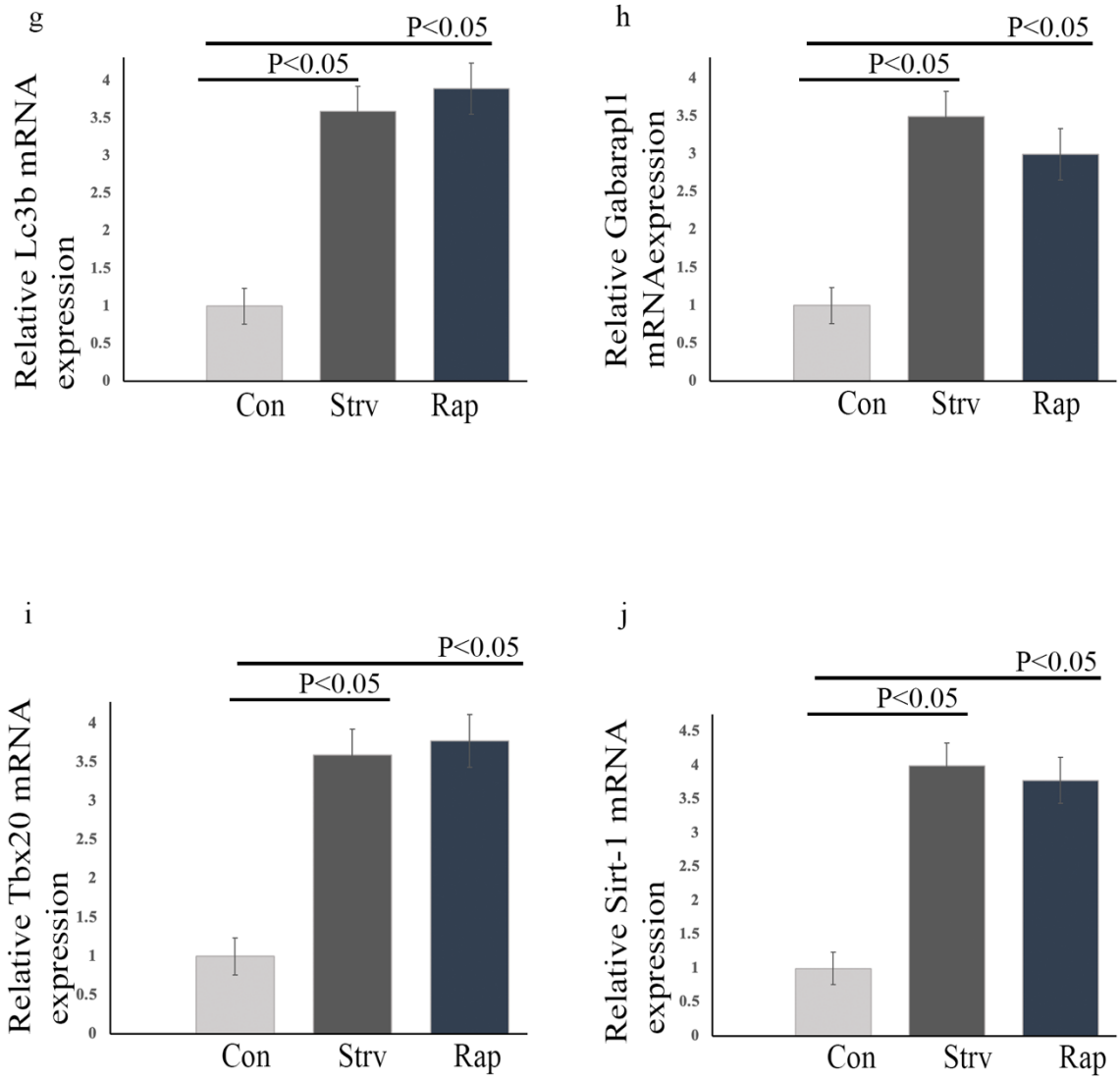

[*Figure 1: qPCR study of Autophagy induced reactivation of Tbx20 in H9c2 cells and aged mice.* *The reactivated expression of TBx20 along with the expression of Lc3b, Beclin1, gabarapl1, mTORC1 and Sirt1 was assessed with qPCR assay. A 3.8 and 3.7 fold enhanced expression of Lc3b for starvation and rapamycin treated cells confirmed successful autophagy induction following starvation and rapamycin treatment. A 3 and 3.3 fold increase in the expression of Gabarapl-1 and 3 and 2.8 fold increase in the mRNA expression of Beclin1 for starvation and rapamycin cells was found. mTORC1 was found to be inhibited following starvation and rapamycin treatment as 0.55 and 0.36 fold expression was observed compared to the control group. Tbx20 mRNA expression was found to increase by 3 and 3.2 fold in starvation and rapamycin treated groups while*

Sirt1 showed a 3.4 and 3 fold increase for starvation and rapamycin treated groups respectively as compared to the control group. Similarly a 3.6 and 3.9 fold upregulation in Lc3b mRNA levels was observed for mice treated with Strv and Rap respectively. An elevated fold change of 3.3 and 3 was observed for expression of Gabarapl-1 mRNA in Strv and Rap treated mice. The expression of Tbx20 was found to be 3.5 and 3.7 for Strv and Rap tr mice while Sirt1 was found to be upregulated by 3.9 and 3.7 folds in Strv and Rap treated mice respectively in comparison to control group. n=3, $p < 0.05$ was considered statistically significant. Data expressed as mean ± SD. **]**

Autophagy induced reactivation of Tbx20 in H9c2 cells. Tbx20 has recently been known to be reactivated and induced under subjection to cardiac stress conditions and the cardioprotective role it confers.[6,77,111] In our case also, following starvation and rapamycin treatment, Tbx20 expression was found to be significantly upregulated in the H9c2 cells in comparison to the control group validated by both anti-Tbx20 antibody staining and WB (Fig.1a, b and c). Successful induction of autophagy under both treatment conditions was validated by enhanced expression of Lc3-II, Beclin-1 and GSK-3β (Fig. 2c, d, e, f and g) proteins. Beclin-1, one of the important mediators of autophagy responsible for the formation of the autophagosome in the earlier stages of autophagy[20,25]was also assessed via anti-Beclin-1 immunostaining (Fig. 1h and i) and followed the same anticipated pattern of significant overexpression in comparison to the control group. Total protein was used as loading control for WB. Overall the panel shows autophagy-mediated reactivation of Tbx20.

Figure 2

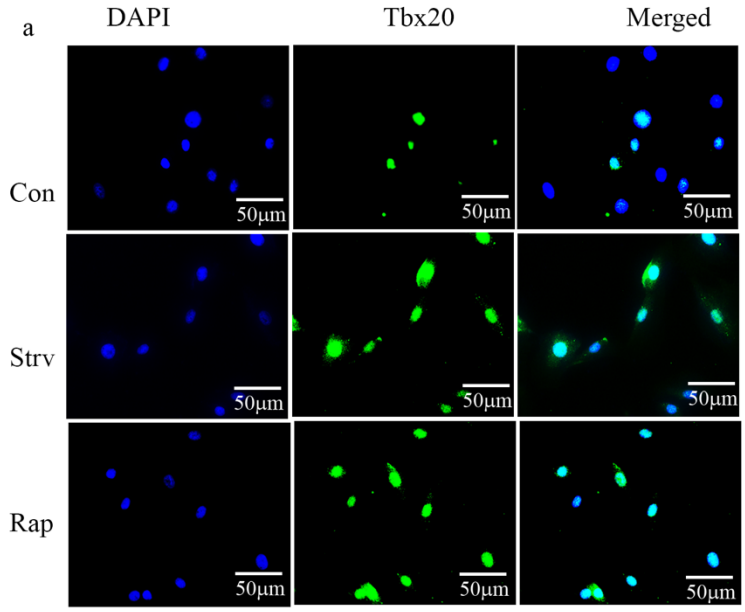
a
DAPI
Tbx20
Merged
Con
Strv
Rap
50μm

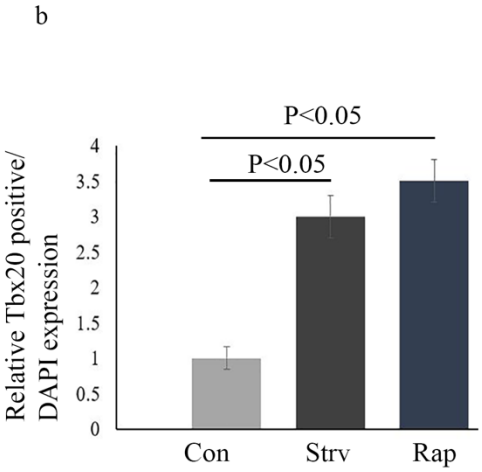
b
P<0.05
P<0.05
Relative Tbx20 positive/ DAPI expression
4
3.5
3
2.5
2
1.5
1
0.5
0
Con
Strv
Rap

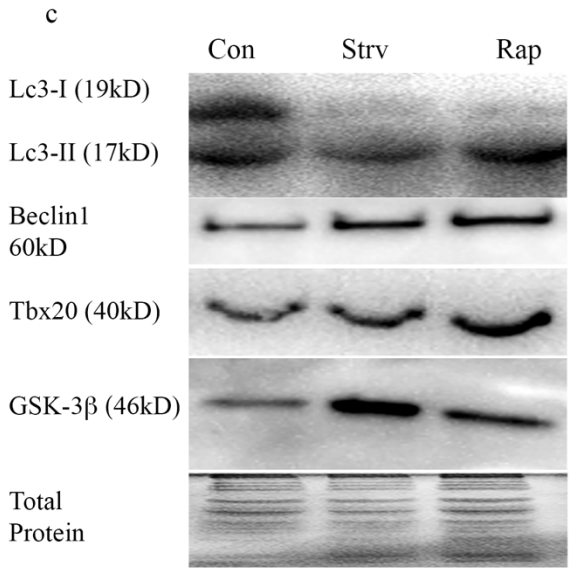
c
Con
Strv
Rap
Lc3-I (19kD)
Lc3-II (17kD)
Beclin1 60kD
Tbx20 (40kD)
GSK-3β (46kD)
Total Protein

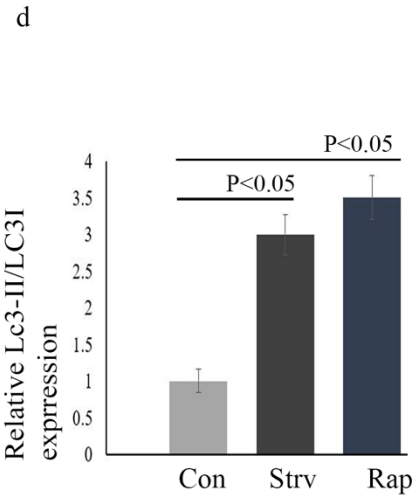
d
P<0.05
P<0.05
Relative Lc3-II/LC3I exprression
4
3.5
3
2.5
2
1.5
1
0.5
0
Con
Strv
Rap

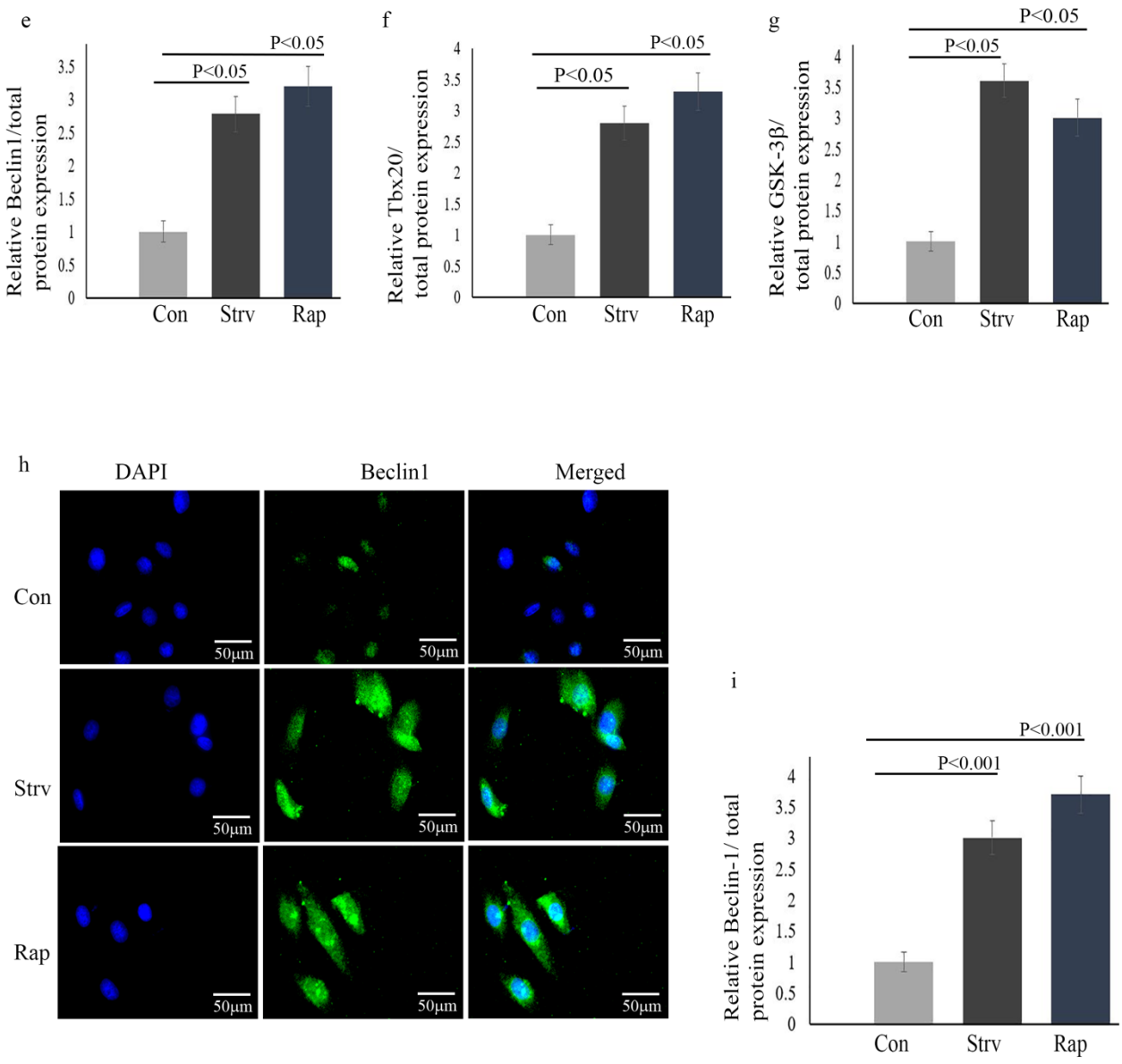

**[*Figure 2: Tbx20 upregulation in H9c2 cells following autophagy induction depicted by IF and WB.* *Tbx20 (shown in green) immunostaining revealed a 3- and 3.5-fold increase in the no. of Tbx20 positive cells for H9c2 cells treated with Strv and Rap respectively (Fig. 3 a, b). Also, WB for Lc3 showed a 2.9 and 3.5 fold increase in the Lc3-II/lc3-I ratio validating successful autophagy induction (c, d). Beclin1 protein was found to be elevated by 2.7 and 3-fold in Strv and Rap treated cells respectively (c, e). Tbx20 WB shows a 2.8 and 3 fold increase in strv and Rap treated cells (c,f) while GSK3β showed a 3,5 and 3 fold increase in cells treated to Strv and Rap respectively (c, g). Beclin1 immunostaining (shown in*

green) also showed a 2.9 and 3.6 fold increase in the fluorescence intensity (h,i). DAPI (shown in blue) was used as nuclear stain. Total protein was used as loading control for WB. n=3 data analysed and expressed as mean ± SD. Differences were considered statistically significant for p < 0.05. **]**

H9c2 proliferation assay. Taking a cue from the well-documented role of Tbx20 in cardiomyocyte proliferation, [2,80,111]proliferation assay was done by Ki67 immunostaining (Fig. 2 a, b) and a significant fall in the expression of Ki67 was observed for Strv and Rap treated cells.

Figure 3

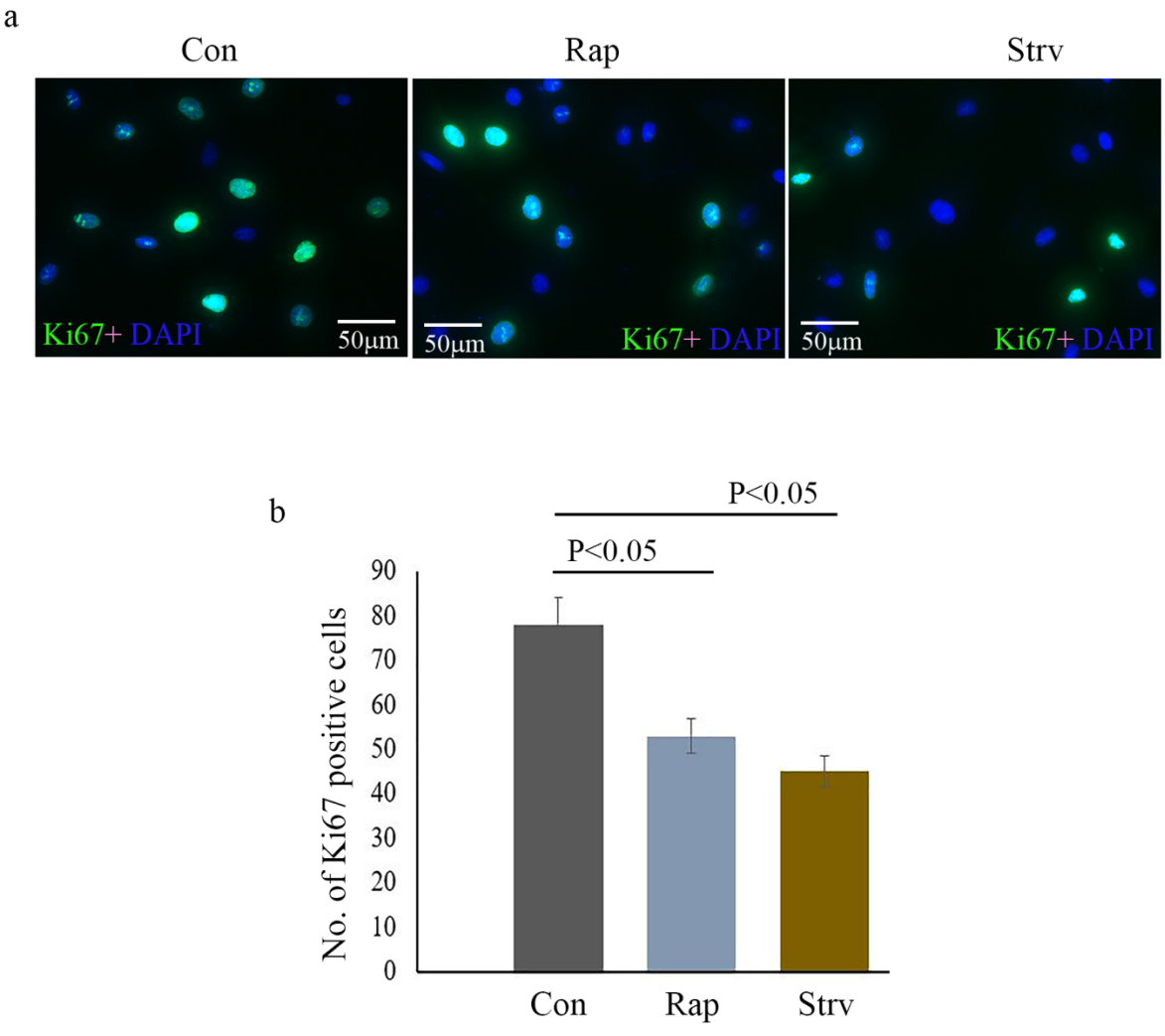

[***Figure 3: H9c2 proliferation assay by Ki67 staining.*** *Ki67 staining (shown in green) depicts karyokinesis and it was found that the number of Ki67 positive cells in both Strv and Rap treated cells declined. The number of Ki67 positive cells were found to be 55 and 45 for Strv and Rap treated cells while 78 in the control group. DAPI, shown in blue was used for staining the nucleus. n=3. data analysed and expressed as mean ± SD. Differences were considered statistically significant for* $p < 0.05$. **]**

Homoeostatic balance between autophagy and apoptosis. Since Ki67 staining showed poor Since proliferation study showed a decline in the proliferative efficiency of starvation and rapamycin treated H9c2 cells, apoptotic markers were assessed to determine whether exacerbated apoptosis is underway following autophagy induction. Both cell viability and apoptotic/necrotic assay were done. While CV450 immunostaining showed in starvation treated H9c2 cells about 75% of cells were viable, less than a quarter of the percentage of rapamycin treated cells were non-viable or metabolically inactive when compared to the control group. Similarly, Apoxin green and 7-AAD antibody staining reflected that while very few cells in the control group were found to be apoptotic and even less necrotic, starvation and rapamycin treated cells did show enhanced but a not alarming expression of Apoxin green and also that of 7-AAD to some extent. H9c2 cells treated with Paclitaxel (80 nM) for 12 hours were used as a positive control for the apoptotic assay, since paclitaxel has long been known to be an apoptosis inducer, mediating through Caspase-3 and Caspase- 9.[109] Overall, this is in concordance with the norm of autophagy where some amount of apoptosis is prevalent to recycle and provide for the nutrients required for cellular survival under caloric restriction.

Figure 4

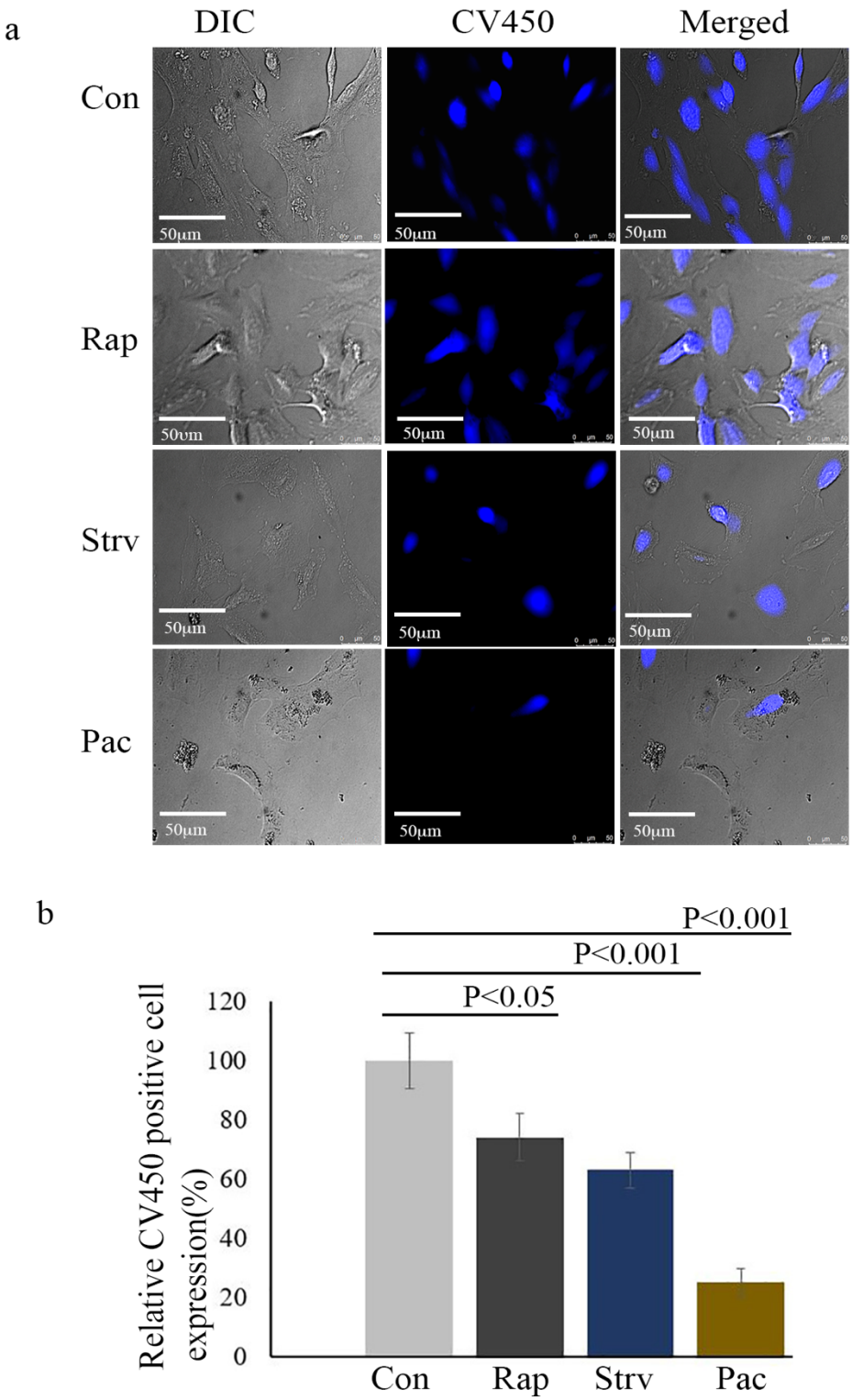
a
DIC
CV450
Merged
Con
Rap
Strv
Pac
50μm
b
P<0.001
P<0.001
P<0.05
Relative CV450 positive cell expression(%)
120
100
80
60
40
20
0
Con
Rap
Strv
Pac

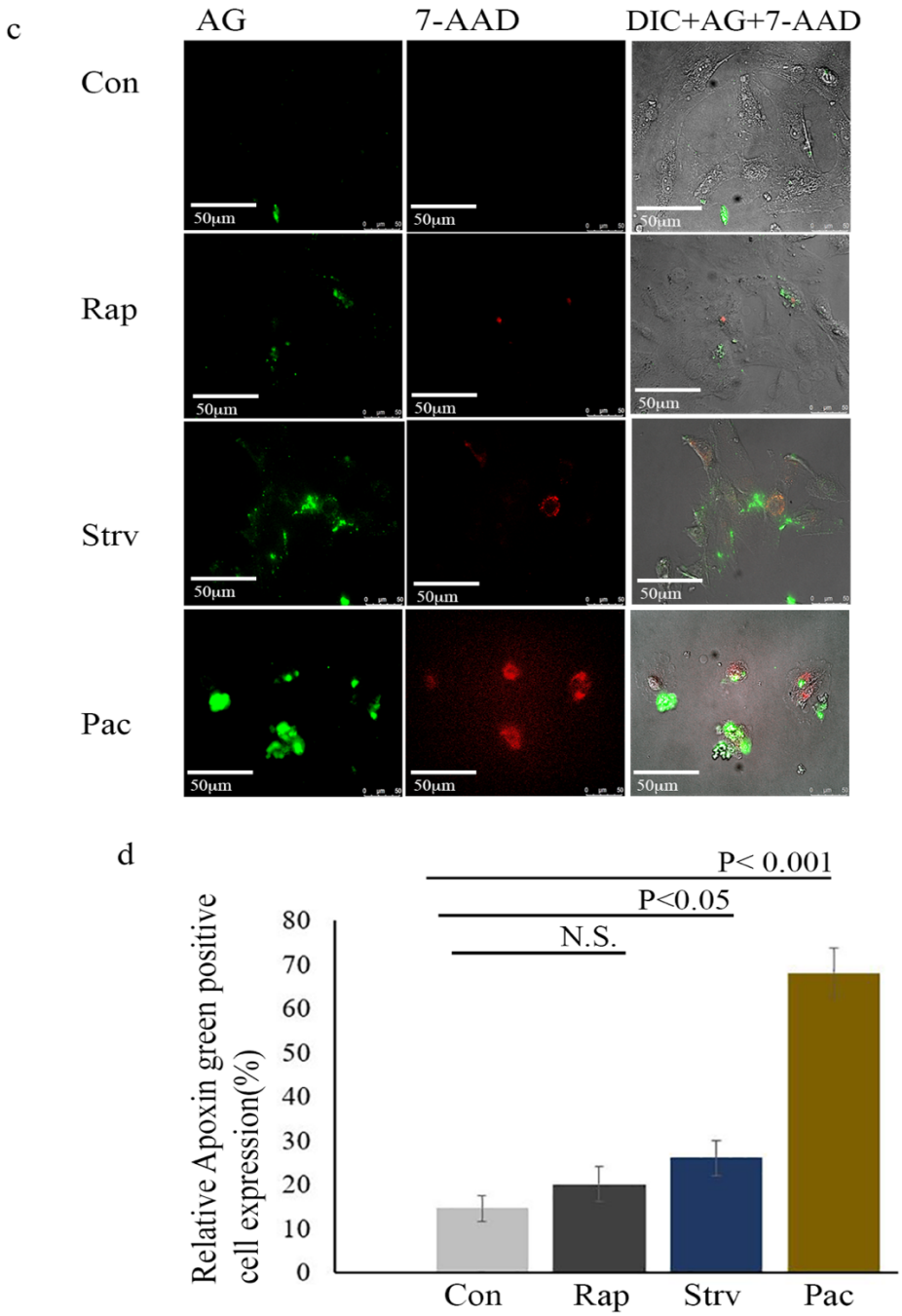

[*Figure 4: Detection of apoptosis rate under autophagy influence.* *Staining with CV450 (blue) showed decline in cellular viability in both starvation and rapamycin treated cells. The relative no of H9c2 cells found to express CV450 was 78% and 70% in Rap and Strv treated groups respectively compared to control whereas only 30% cells were found to be viable in the Pac treated group (a and b). For observing cellular morphology DIC images were also taken.*

Further, staining with AG (shown in green)and 7-AAD (shown in red) showed increase in the extent of apoptosis and necrosis in the Strv and Rap treatment group in comparison to the control group even though only a few necrotic cells were observed in the treatment group. The ratio of apoptotic/necrotic cells observed were found to be 20% in control group, 30% and 40% in strv group. Cells treated with Pac showed highest apoptosis at 75% (c and d). n=3. Data analyzed and expressed as mean ± SD. Differences were considered statistically significant for $p < 0.05$. Difference between Strv and Rap treatment groups were found to be non-significant. **]**

In-silico interaction study between Tbx20 and Sirt1 DNA

In silico analysis was performed to predict the possibility of binding between T-box site of Tbx20 protein and promoter region of Sirtuin 1 (Sirt1) DNA. Screening through the sequence of Sirt1 from both *Rattus norvegicus* (NCBI ref. no. NM_01372090.1) and *Mus musculus* (NCBI ref. no. NM_019812.3) revealed the presence of a consensus T-box binding sequence AGGTGTGA[112] (Fig. 5a, b) 600 bps upstream of the coding region of Sirt1. This palindromic sequence is known as the T/2 sites[113] that is generally found in the natural promoters of all the target genes for T-box transcription factors.

Figure 5

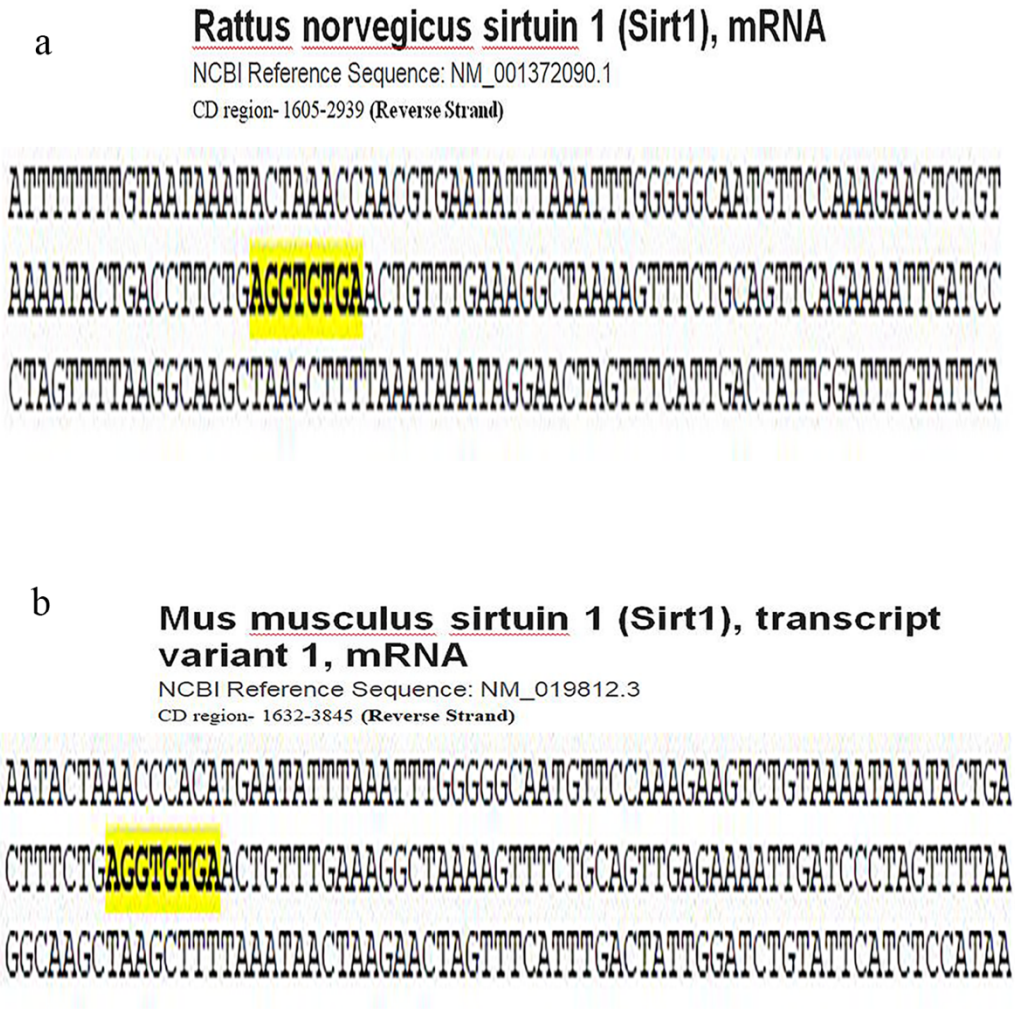

[***Figure 5: Tbx20-Sirt1 interaction in-silico assay.*** *Pair wise sequence alignment was then performed taking these Sirt1 sequences from both the organisms. A 20bp stretch of DNA that is conserved in both the organisms and contains the consensus T-box binding sequence was thus selected as the possible substrate DNA (panel a and b) where Tbx20 can bind. The reverse DNA strand of Sirt1 specific to both Mus musculus and Rattus norvegicus was found to contain all 8 matching nucleotide bases. The matching region was identified upstream of CD complement region in both the genus. The CD complement region for Mus musculus was recognised from 1632-3845 bp position and the target site containing 5'-AGGTGTGA-3'was identified at 500bp position while*

the CD complement region in Rattus norvegicus was shown to range from 1605-2939 while the same matching sequence site, 5'-AGGTGTGA-3' was found at around 550 bp position i.e., about 1000bp upstream of DNA. **]**

Cell size determination of mice treated with Strv and Rap. WGA staining (WGA being a lectin binding protein binds to the glycoproteins in the cell membrane and thus labels the cell membrane) with heart tissue section of mice treated with Strv and Rap was performed and no significant difference in cell sizes were found (measured with the help of imageJ was noticed).

Figure 6

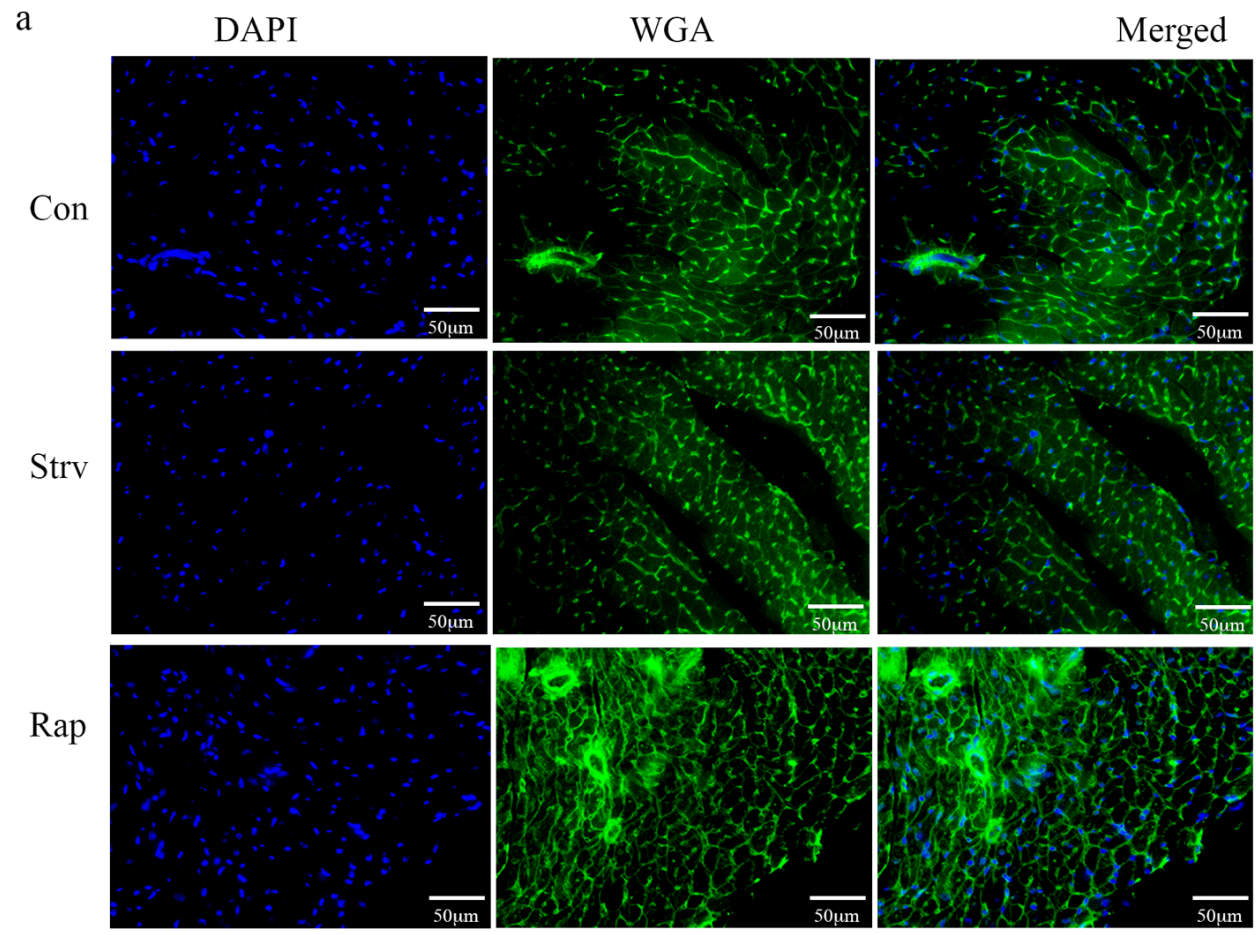

[***Figure 6: Assessment of cell size in heart tissue samples of mice treated with Strv and Rap.*** *WGA staining (shown in green) was done to mark the cell size. No*

noticeable and significant difference in cell size was observed among the groups. DAPI was used as nuclear stain. n=3, p > 0.05. **]**

Autophagy mediated activation of Nkx2.5, Gata4, Sirt1, GSK-3β in addition to Tbx20 in aged murine hearts. Consistent with the in-vitro findings here also, Tbx20 protein expression was significantly increased in both starvation and rapamycin treated male, aged Swiss albino mice shown by Tbx20 WB (fig. 7 a and d). Successful induction of autophagy was validated by elevated expression of Lc3-II/Lc3-I ratio, Beclin-1as demonstrated by protein blots (Fig. 7a, b and c). GSK-3β , also a known activator of autophagy[20] was also significantly upregulated in both the treatment groups compared to the control group (Fig 6a and g) and interestingly p- GSK-3β form was downregulated in aged mice that were subjected to autophagy induction (Fig 7a). Additionally, GSK-3β has also recently come under light for its cardioprotective and cardiac homeostasis maintenance role.[114] Besides being an important factor in aging and higher levels of p-GSK-3β is found to increase with age progression and conversely, poor levels of active GSK-3β are in the protein pool.[115,116] Low levels of GSK-3β has been linked with cardiac senescence. Finally, transcription factors Nkx2.5 and Gata4 were also upregulated following autophagic induction (Fig 7a, e and f). Last but not least Sirt1 protein levels were significantly upregulated in both starved and rapamycin treated aged mice (Fig. 7a, h). This finding is indicative of the already established role of Sirt1 in cardiac senescence and its upregulation following caloric restriction alone has been shown to improve cardiac health and longevity. Overall, this suggests that Tbx20 might be regulating GSK-3β and Sirt1 in addition to Nkx2.5 and Gata4 based on the bioinformatic tool and in-vivo findings.

Figure 7

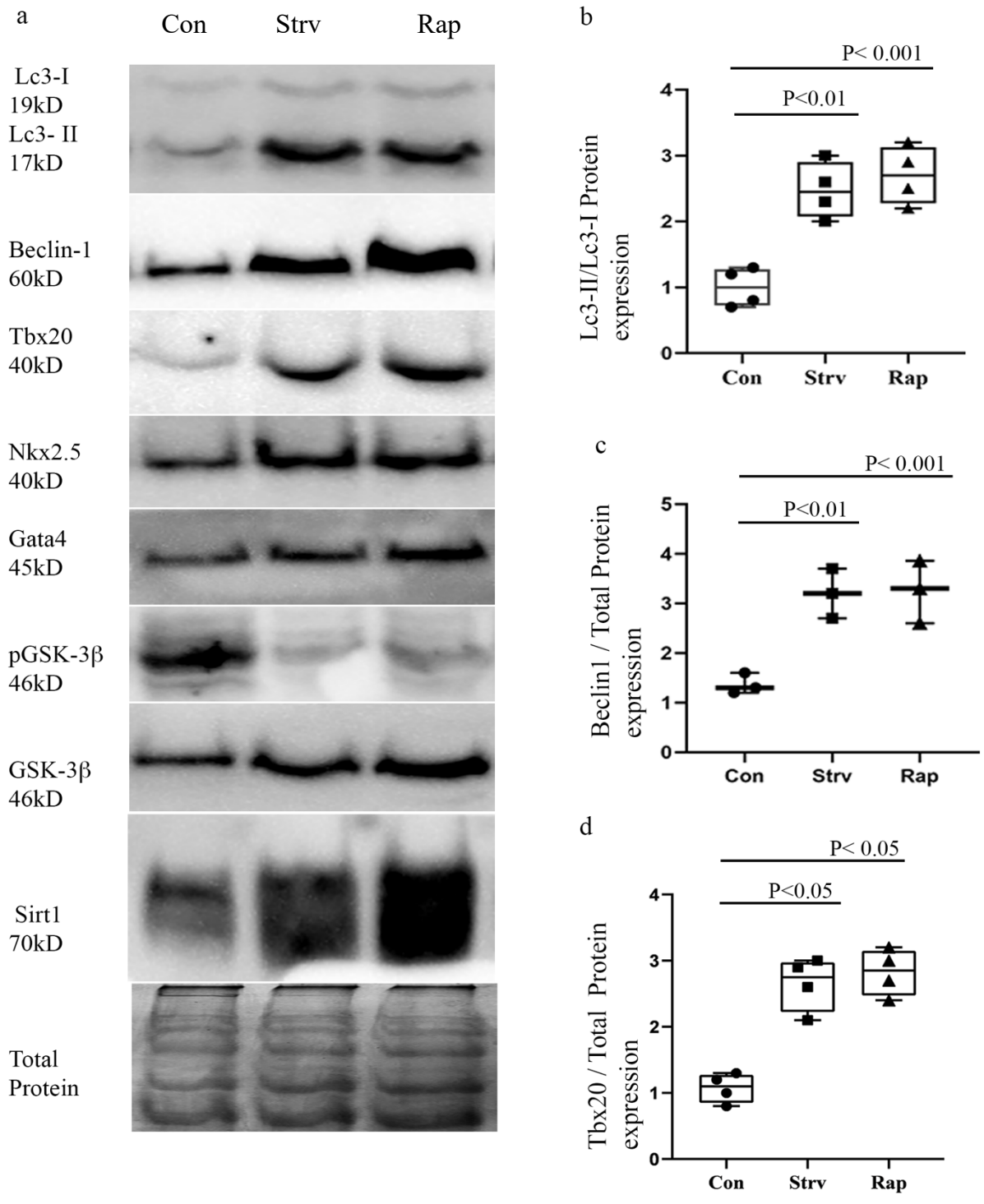
a
Con
Strv
Rap
Lc3-I
19kD
Lc3- II
17kD
Beclin-1
60kD
Tbx20
40kD
Nkx2.5
40kD
Gata4
45kD
pGSK-3β
46kD
GSK-3β
46kD
Sirt1
70kD
Total
Protein
b
P< 0.001
P<0.01
Lc3-II/Lc3-I Protein expression
Con
Strv
Rap
c
P< 0.001
P<0.01
Beclin1 / Total Protein expression
Con
Strv
Rap
d
P< 0.05
P<0.05
Tbx20 / Total Protein expression
Con
Strv
Rap

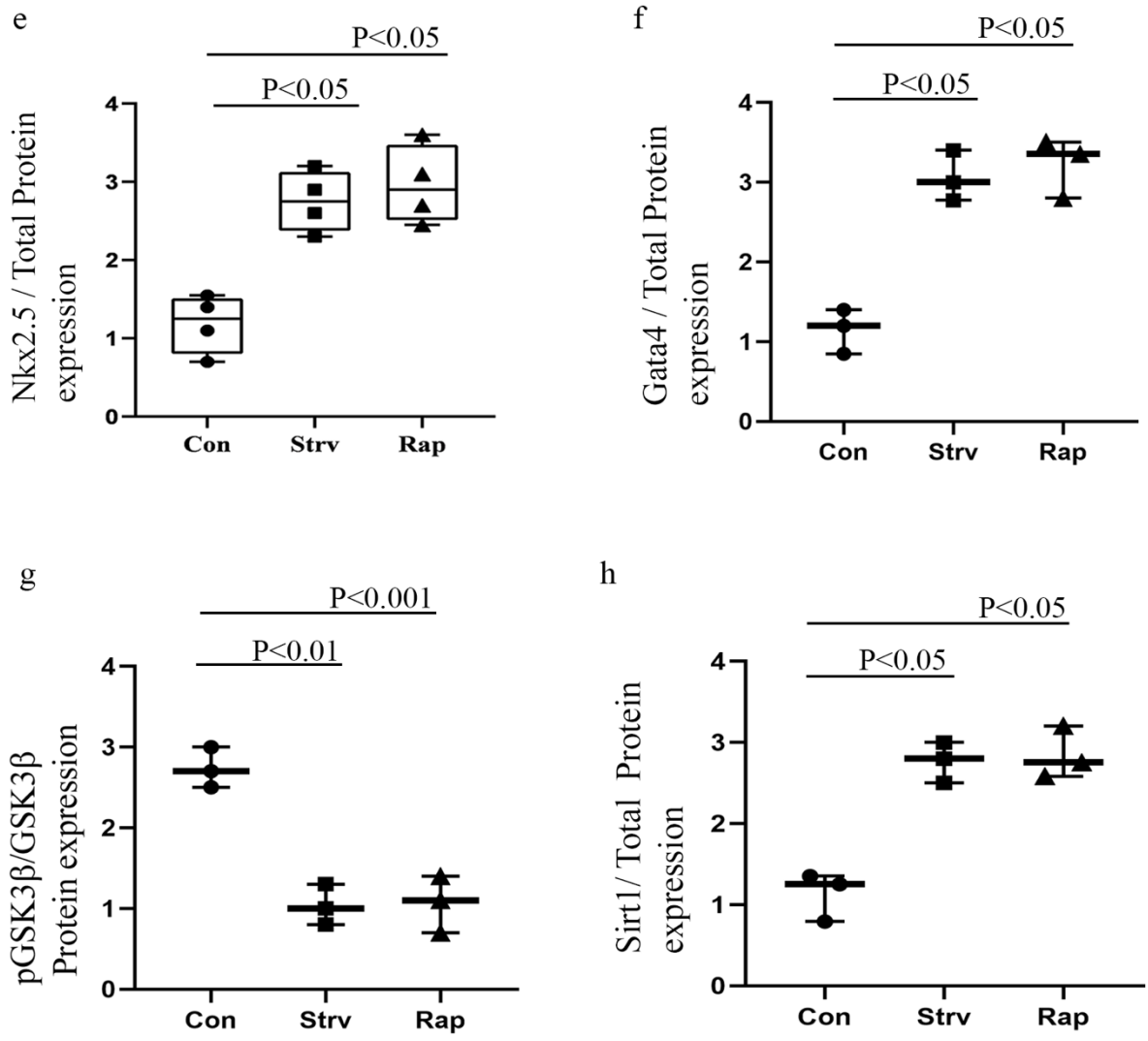

[*Figure 7: In-vivo expression of TBx20 along with GSK-3β, Sirt1, Nkx2.5 and Gata4 after Strv and Rap treatment.* *WB for Lc3, Beclin1, Tbx20, Nkx2.5, Gata4, pGSK3β, GSK3β, Sirt1 was performed (a) for mice treated with Strv and Rap along with control group. Lc3-II/Lc3-I was found to 2.5 and 2.7-fold elevated in comparison to this control group (b), Beclin-1 was found to be elevated by 3 and 3.3 folds in Strv and Rap tr models respectively while Tbx20 was increased by 2.7 and 2.9 folds in Strv and Rap tr groups in comparison to control group (Fig 1 d). Nkx2.5 protein levels increased by 2.8 and 3.2 folds in Strv and Rap treated groups respectively. Gata4 also was found to increase by 3 and 3.3 folds in both the experimental groups. pGSK3β/GSK3β (h) was found to be 1 and 0.9 in Strv and Rap tr groups respectively and lastly Sirt1 levels were elevated by 2.9 and*

3.3 folds in Strv and Rap tr aged mice (h). Total protein was used as loading control for WB. n= at least 3, data analysed and expressed as median ± SD. Differences were considered statistically significant for $p < 0.05$. **]**

Autophagy regulation through mTORC1 and upregulation of Tbx20 and Sirt1 in aged mice. Autophagy induction in aged murine hearts was mediated through mTORC1. IHC with anti-mTORC1 antibody was done and the significant decline in the expression of mTORC1 in both the starvation and rapamycin treated groups confirmed this hypothesis (Fig. 8a, b).In addition to Tbx20 and Sirt1 WB, anti-Tbx20 and anti-Sirt1 co-labelled IHC was performed and the no of colocalised Tbx20 and Sirt1 was significantly upregulated in both the treatment groups. (Fig. 8c, d and e). Overall, this is in accordance with our WB findings and depicts that autophagy induction is regulated in a mTORC1 dependent fashion.

Figure 8

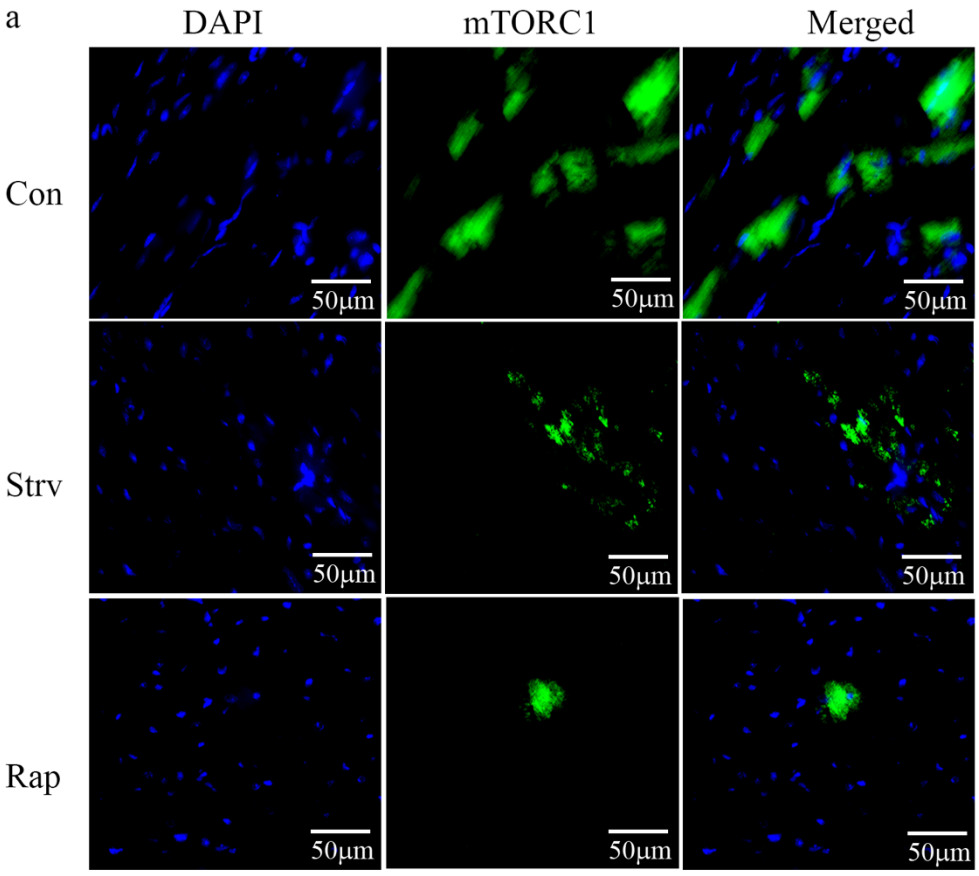
a
DAPI
mTORC1
Merged
Con
Strv
Rap
50μm

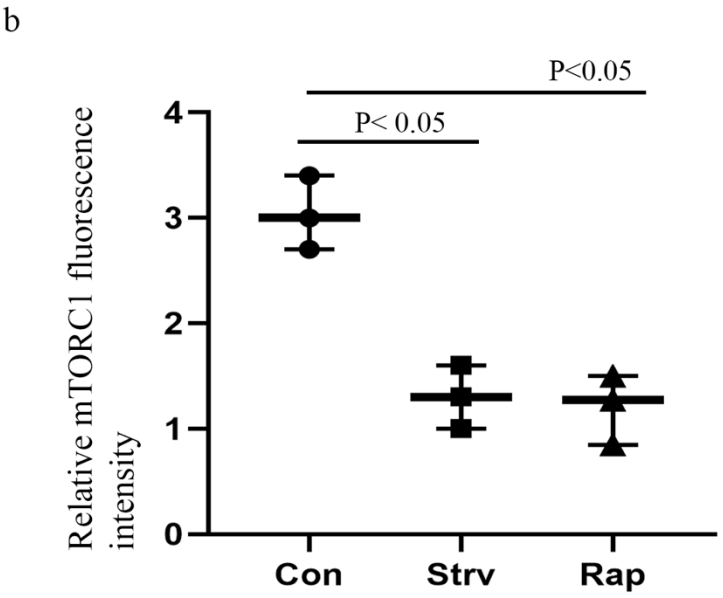
b
P<0.05
P< 0.05
Relative mTORC1 fluorescence intensity
4
3
2
1
0
Con
Strv
Rap

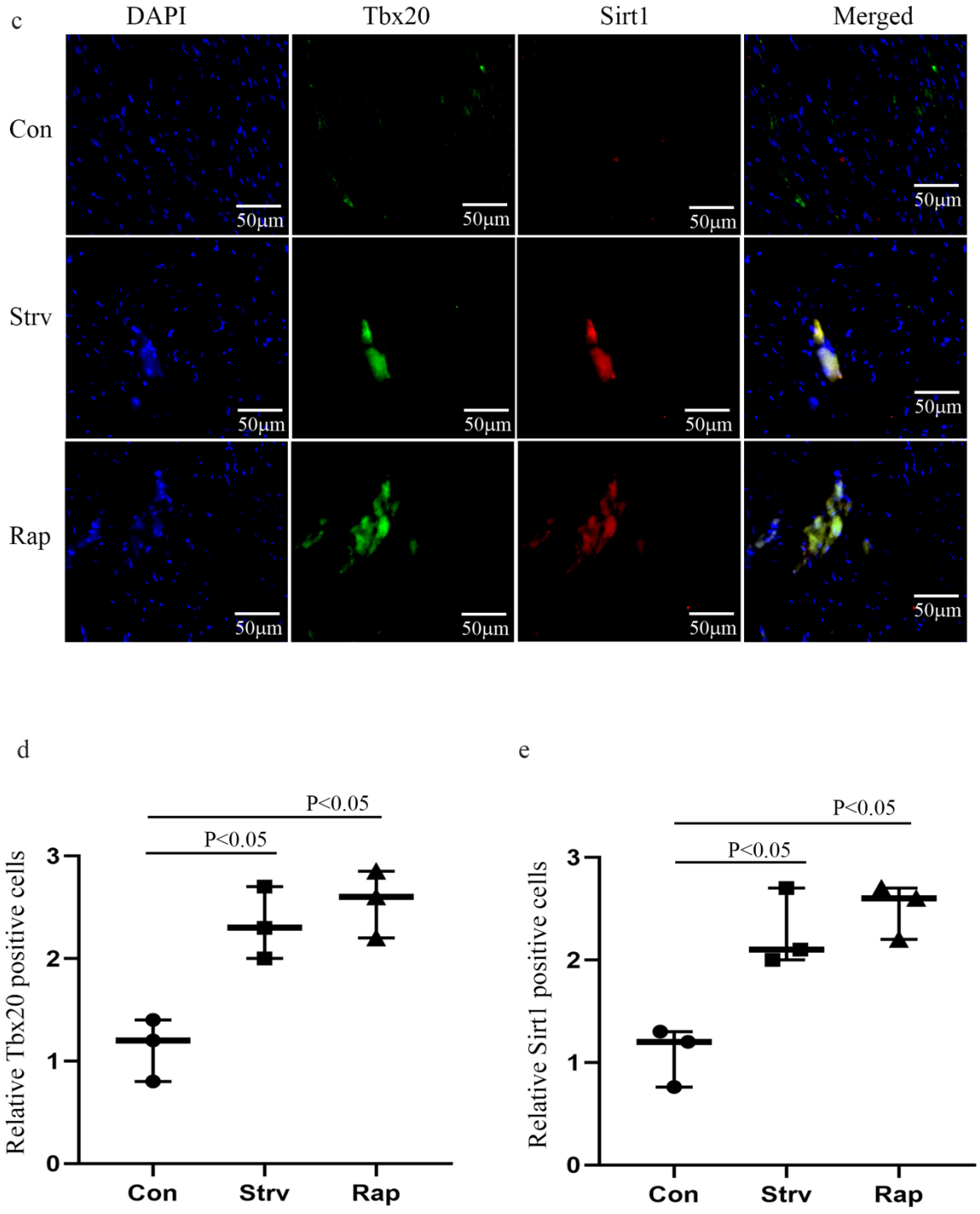

[*Figure 8:Autophagy regulation through mTORC1 and upregulation of Tbx20 and Sirt1 in aged mice.* *IHC of mice heart sections with mTORC1 antibody (shown in green) showed a reduction to 1.5 and 1.4 fold for Strv and Rapamycin treated mice from that of 3 fold observed for the control group (a and c) depicts*

successful authophagy induction is mTORC1 mediated. Further co-labeled IHC with Tbx20 (shown in green) and Sirt1 (shown in red) (b) shows co-localised expression of Tbx20 and Sirt1 and an enhanced median expression of 2.3 and 2.6 fold for Strv and Rap treated mice for Tbx20 positive cells as compared to the control group. Similarly, Sirt1 showed a 2.2 and 2.4 fold increment in the number of Sirt1 positive cells (b and d). DAPI (shown in blue) was used as nuclear stain. n=3, data analysed and expressed as median ± SD. Differences were considered statistically significant for $p < 0.05$. **]**

High levels of GSK-3β and low levels of p-GSK-3β found in aged murine hearts following autophagy induction. Further along, IHC with anti-GSK-3β and anti -pGSK-3β antibodies were done with mice heart sections. It showed the enhanced expression of GSK-3β in both starved and rapamycin administered mice and at the same time, lower levels of pGSK-3β in these groups were observed in comparison to the control aged group (Fig 9 a, b). These findings align with reports that state the enhanced expression of pGSK-3β is responsible for cardiac senescence as is the case with the aged control group and a lower ratio of GSK-3β / pGSK-3β is beneficial for improved cardiac health which is what we have found in both the treated groups.

Figure 9

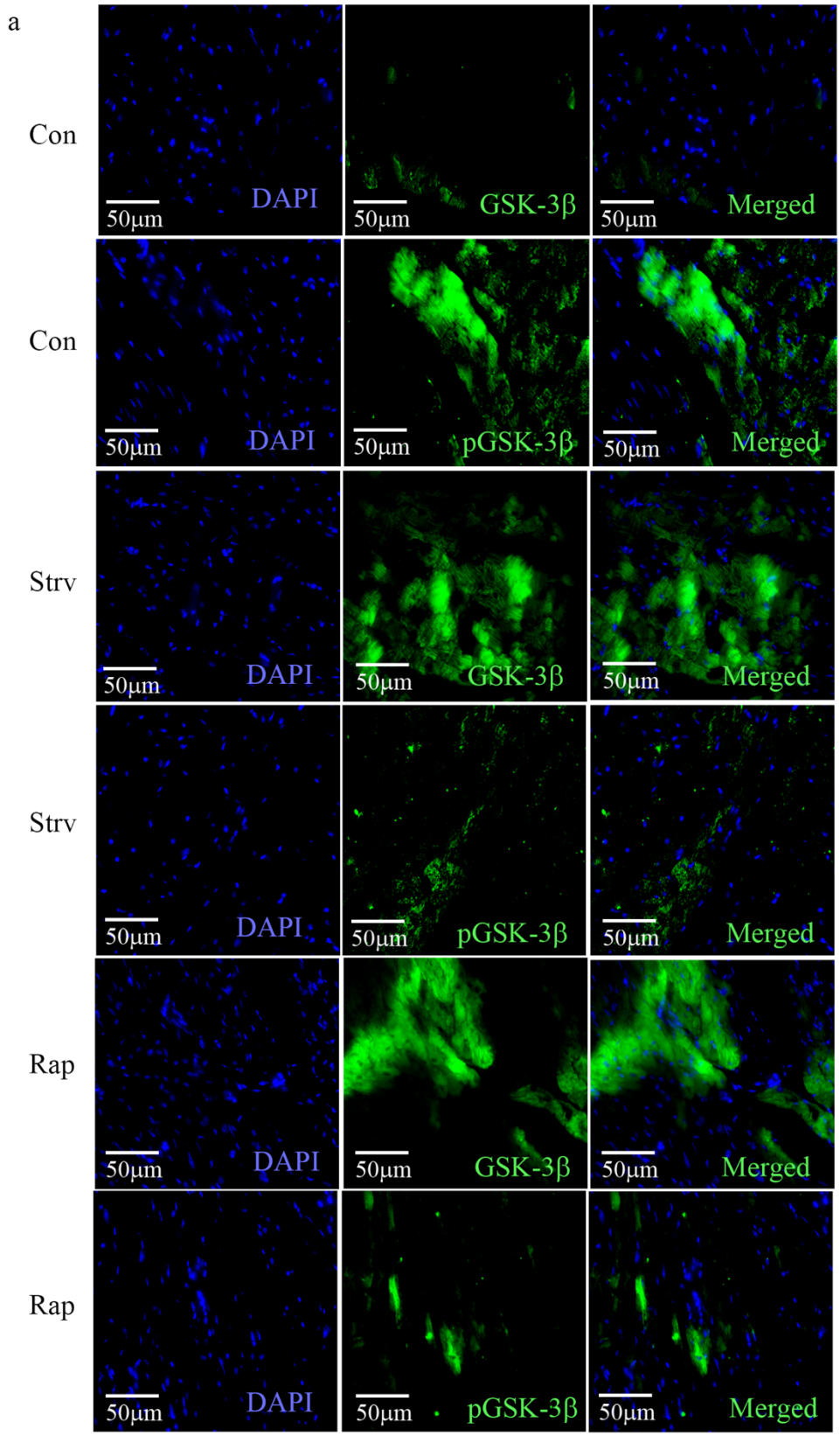
a
Con
DAPI
GSK-3β
Merged
Con
DAPI
pGSK-3β
Merged
Strv
DAPI
GSK-3β
Merged
Strv
DAPI
pGSK-3β
Merged
Rap
DAPI
GSK-3β
Merged
Rap
DAPI
pGSK-3β
Merged
50μm

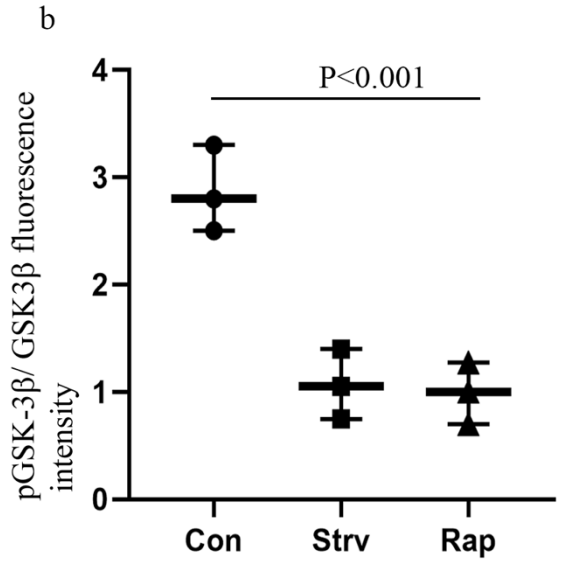

[***Figure 9: High levels of GSK-3β and low levels of p-GSK-3β found in aged murine hearts following autophagy induction.*** *A higher level of GSK-3β was observed in mice treated with Strv or Rap whereas its phosphorylated form was found to be pre-dominant in control group. Immunostaining with GSK-3β and p-GSK-3β (both shown in green) in mice heart sections shows a high p- GSK-3β/ GSK-3β expression in the control group- a 3.1 fold vs the 1.3 and 1.2 fold expression observed for Strv and Rap treated mice. n=3, data analysed and expressed as median ± SD. Differences were considered statistically significant for p < 0.05* **]**

In-vitro assessment of GSK-3β expression and Tbx20 LOF assay. The same expression pattern of GSK-3β and pGSK-3β was observed in H9c2 cells (Fig. 10a, b) after starvation and rapamycin treatment as observed in-vivo i.e., higher levels of GSK-3β and suppressed expression of pGSK-3β. To finally assess the Tbx20 mediated regulatory induction of Nkx2.5, Gata4, Sirt1 and GSK-3β Tbx2O LOF assay was performed. Tbx20 siRNA mediated knockdown was performed and successful validation of knockdown was confirmed by Tbx20

antibody staining (Fig. 10c, d), Tbx20 WB (Fig. 10 e, f) both of which showed a 60% reduction in Tbx20 expression.

Figure 10

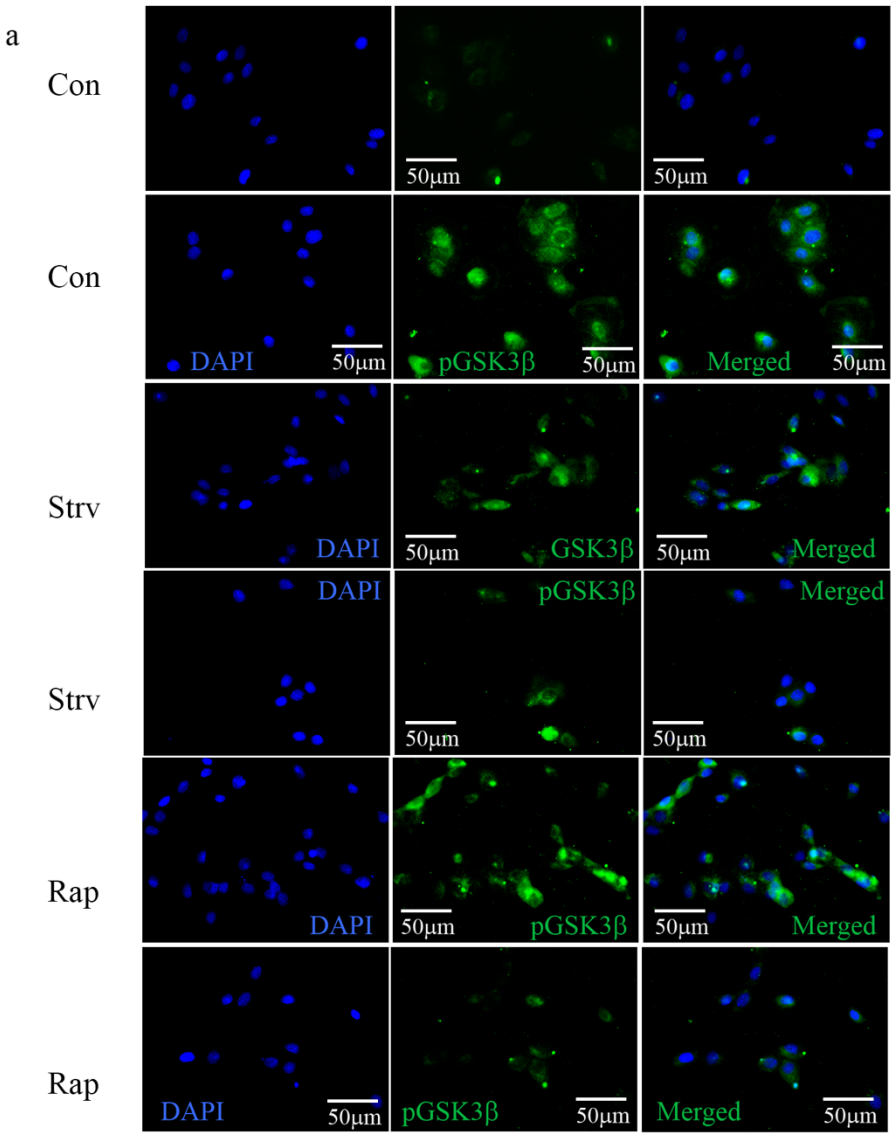
a
Con
Con
Strv
Strv
Rap
Rap
DAPI
pGSK3β
GSK3β
Merged
50μm
b
P<0.05
P<0.05
Relative pGSK-3β/GSK-3β
1.2
1
0.8
0.6
0.4
0.2
0
Con
Strv
Rap

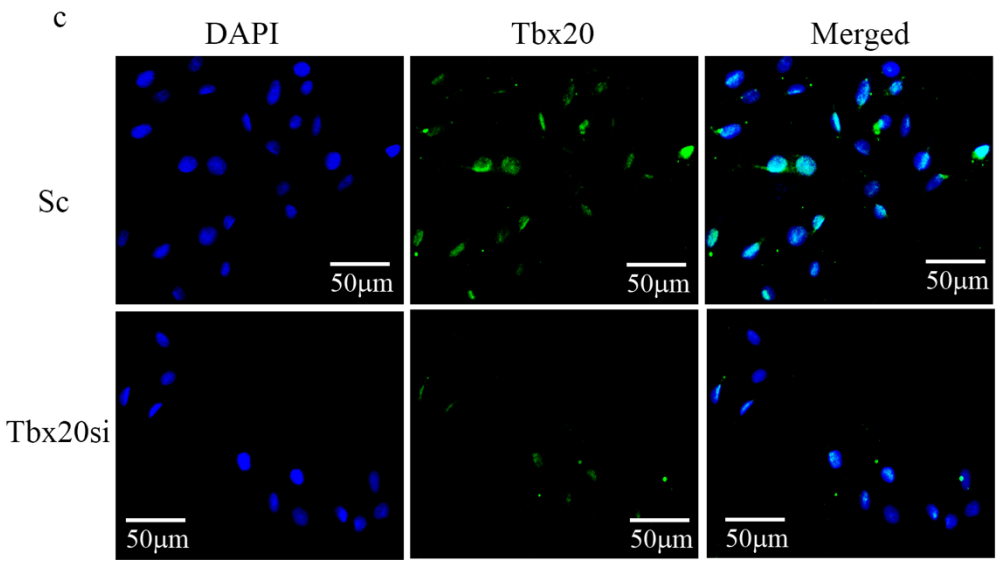
c
DAPI
Tbx20
Merged
Sc
Tbx20si
50µm

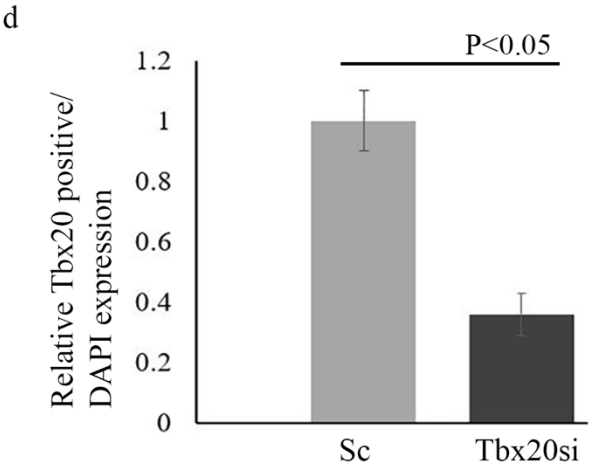
d
P<0.05
Relative Tbx20 positive/ DAPI expression
1.2
1
0.8
0.6
0.4
0.2
0
Sc
Tbx20si

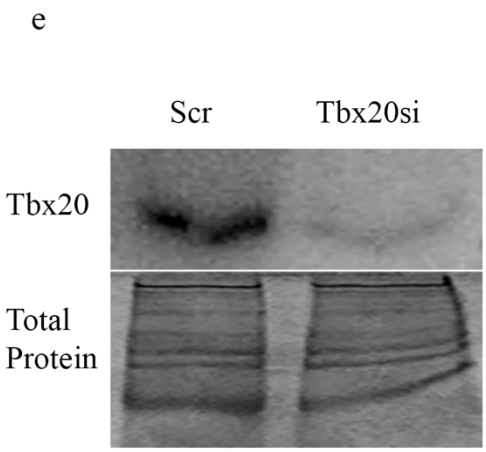
e
Scr
Tbx20si
Tbx20
Total Protein

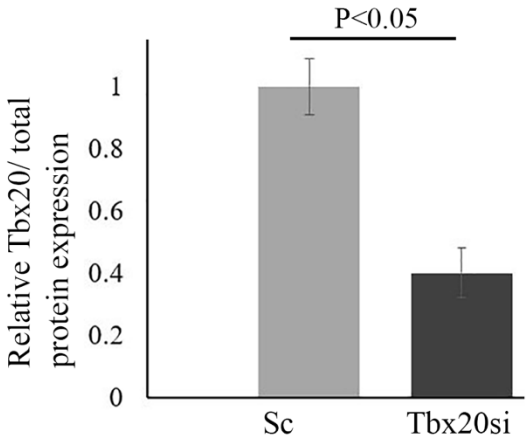
f
P<0.05
Relative Tbx20/ total protein expression
1
0.8
0.6
0.4
0.2
0
Sc
Tbx20si

[***Figure 10: In-vitro assessment of GSK-3β expression and Tbx20 LOF assay.*** *GSK-3β and pGSK-3β (both shown in green) immunostaining showed an elevated expression of GSK-3β in Strv and Rap treated H9c2 cells and a reduction in the expression of pGSK-3β in comparison to the control group (a). pGSK-3β/GSK-3β ratio was reduced to 0.5 and 0.4 folds in Strv and Rap treated groups respectively (a, b). Tbx20 knockdown was assessed by Tbx20 immunostaining (shown in green) (c). The no of Tbx20 positive cells was reduced by almost 60% in the Tbx20si group in comparison to the Sc group. DAPI was used as nuclear stain (shown in blue) Tbx20 LOF was also validated by WB (e, f) which also showed a reduced 0.4-fold expression in the Tbx20si group in comparison to the Sc group. Total protein was used as loading control for WB. n=3, data analysed and expressed as mean ± SD. Differences were considered statistically significant for* $p < 0.05$. **]**

Autophagy induced Tbx20 protein regulates the expression of transcription factors Nkx2.5 and Gata4. Both Nkx2.5 and Gata4 expression were found to be upregulated significantly after starvation and autophagy treatment in H9c2 (Fig. 11a, b, c and d) cells hinting the reactivated function of Nkx2.5 as an activator of cellular proliferation and generation and differentiation of cardiac progenitor pool.[8,117]Gata4 also has been long known to be a marker of cardiac progenitor cell population[118] Upregulated expression of Gata4 and Nkx2.5 proteins indicates the generation of cardiac progenitor pool following autophagy induction. LOF assay of Tbx20 showed a significant drop in the expression of both Nkx2.5 and Gata4 further validating the already established Tbx20 mediated regulation of the latter genes.[102]

Figure 11

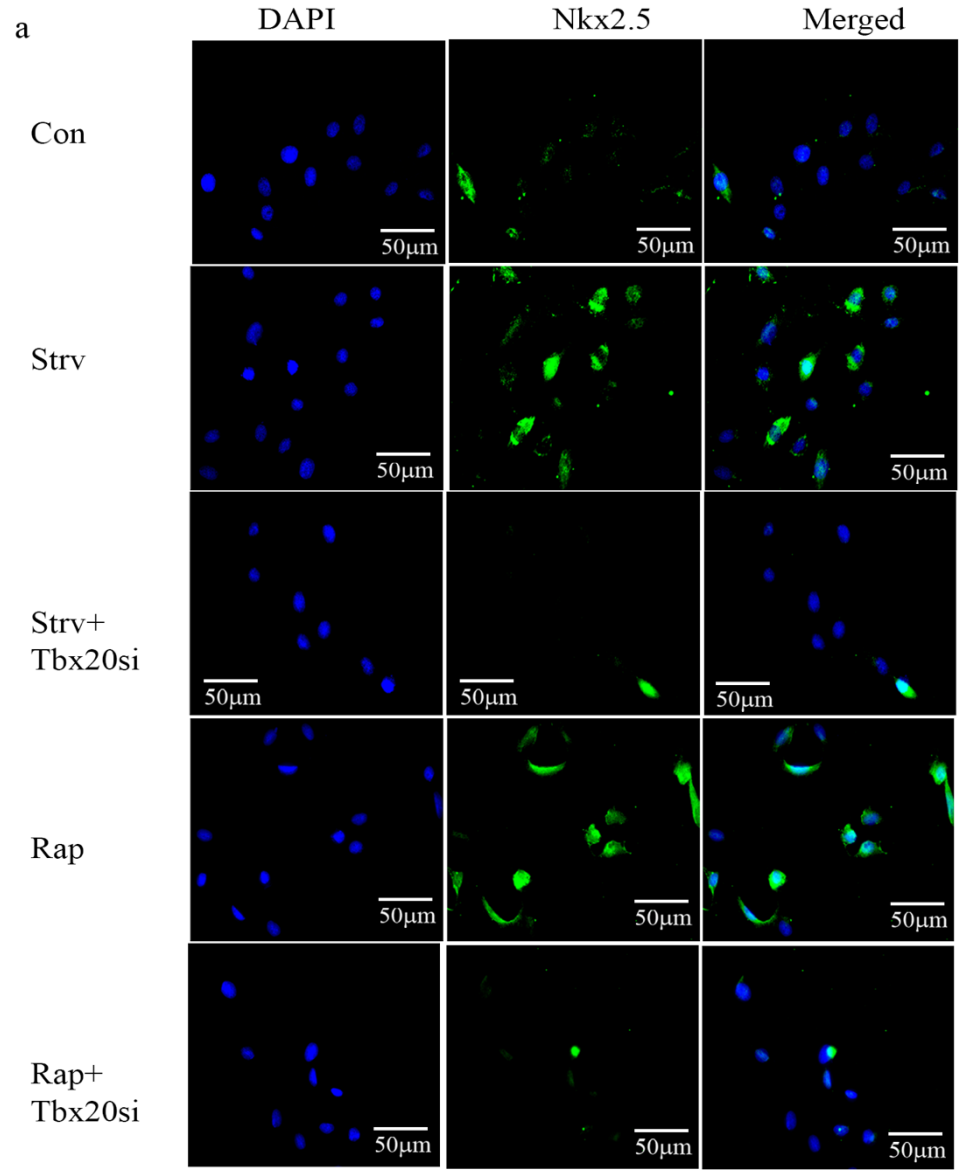
a
DAPI
Nkx2.5
Merged
Con
Strv
Strv+
Tbx20si
Rap
Rap+
Tbx20si
50μm

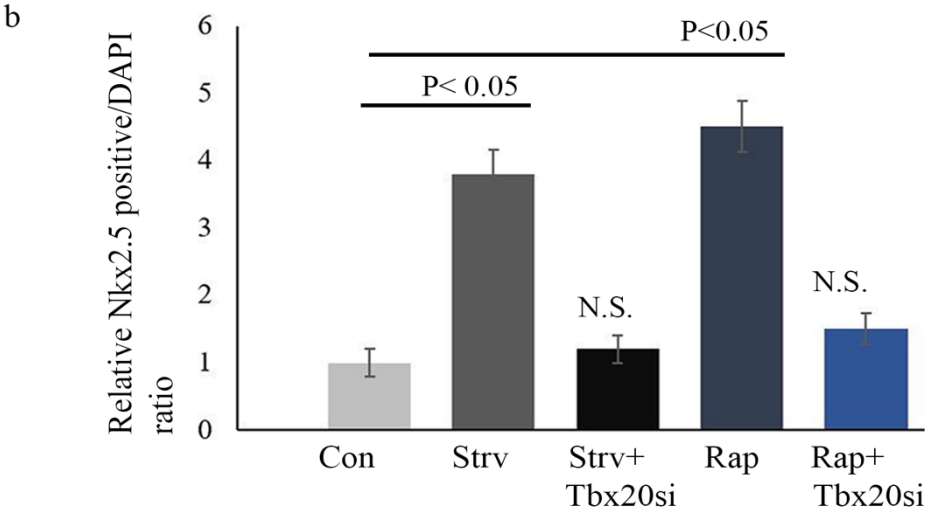
b
Relative Nkx2.5 positive/DAPI ratio
0
1
2
3
4
5
6
P<0.05
P< 0.05
N.S.
N.S.
Con
Strv
Strv+
Tbx20si
Rap
Rap+
Tbx20si

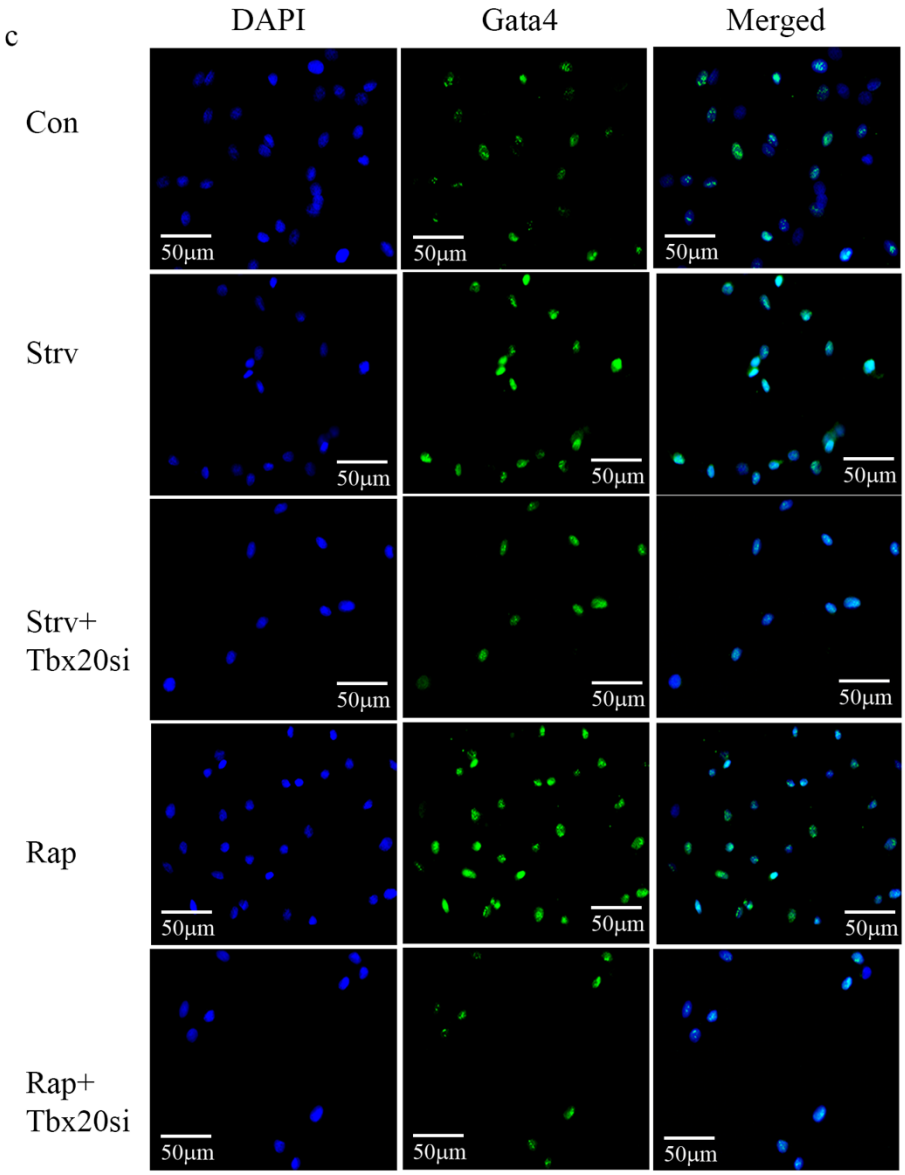
c
DAPI
Gata4
Merged
Con
Strv
Strv+
Tbx20si
Rap
Rap+
Tbx20si
50μm

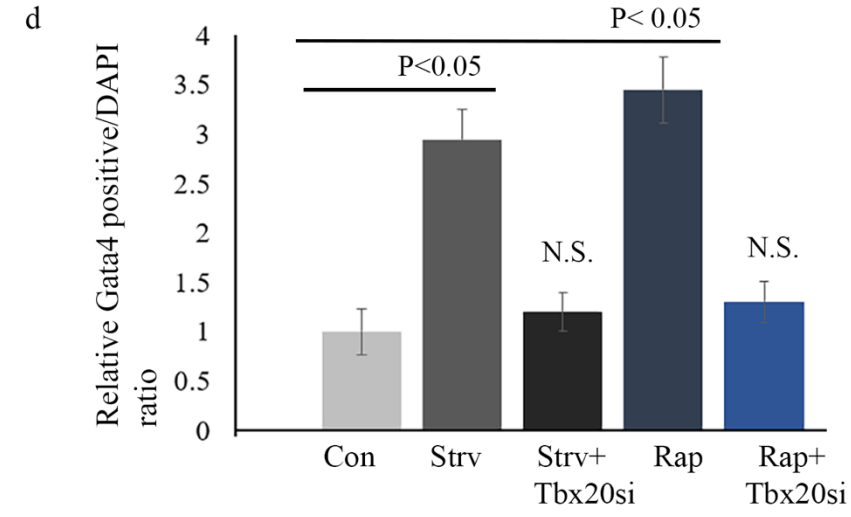
d
Relative Gata4 positive/DAPI ratio
4
3.5
3
2.5
2
1.5
1
0.5
0
P< 0.05
P<0.05
N.S.
N.S.
Con
Strv
Strv+
Tbx20si
Rap
Rap+
Tbx20si

[***Figure 11****: **Tbx20 dependent expression of Nkx2.5 and Gata4.** Staining with anti-Nkx2.5 and anti-Gata4 antibodies (both shown in green) (a and b) show a Tbx20 dependent expression. The 3.8 and 4.2 fold increase in the relative no of Nkx2.5 positive cells for Strv and Rap treated H9c2 cells significantly reduced to 1.2 and 1.5 fold for Strv+Tbx20si and Rap+Tbx20si groups respectively (b). Similarly, the relative no of Gata4 positive cells reduced to 1.2 and 1.4 for Strv+Tbx20si and Rap+Tbx20si cells from 2.8 and 3.4 fold observed for strv and rap treated cells (d). DAPI was used as nuclear stain (shown in blue). n=3, data analysed and expressed as mean ± SD. Differences were considered statistically significant for $p < 0.05$.* **]**

Tbx20 mediated regulation of Sirt1 and GSK-3β under autophagic conditions. The expression pattern of Sirt1 and GSK-3β is aligned with the in-vivo findings mentioned earlier. anti-Sirt1 and anti-GSK-3β antibody staining showed a marked increase in expression of both proteins (Fig. 12 a, b, c and d) following starvation and rapamycin treatment but a marked decline in expression of both the markers was observed after Tbx20 knockdown indicating a regulatory function of Tbx20 in the expression of Sirt1 and GSK-3β. This observation seconds our in-silico finding based on Tbx20 interaction domain.

Figure 12

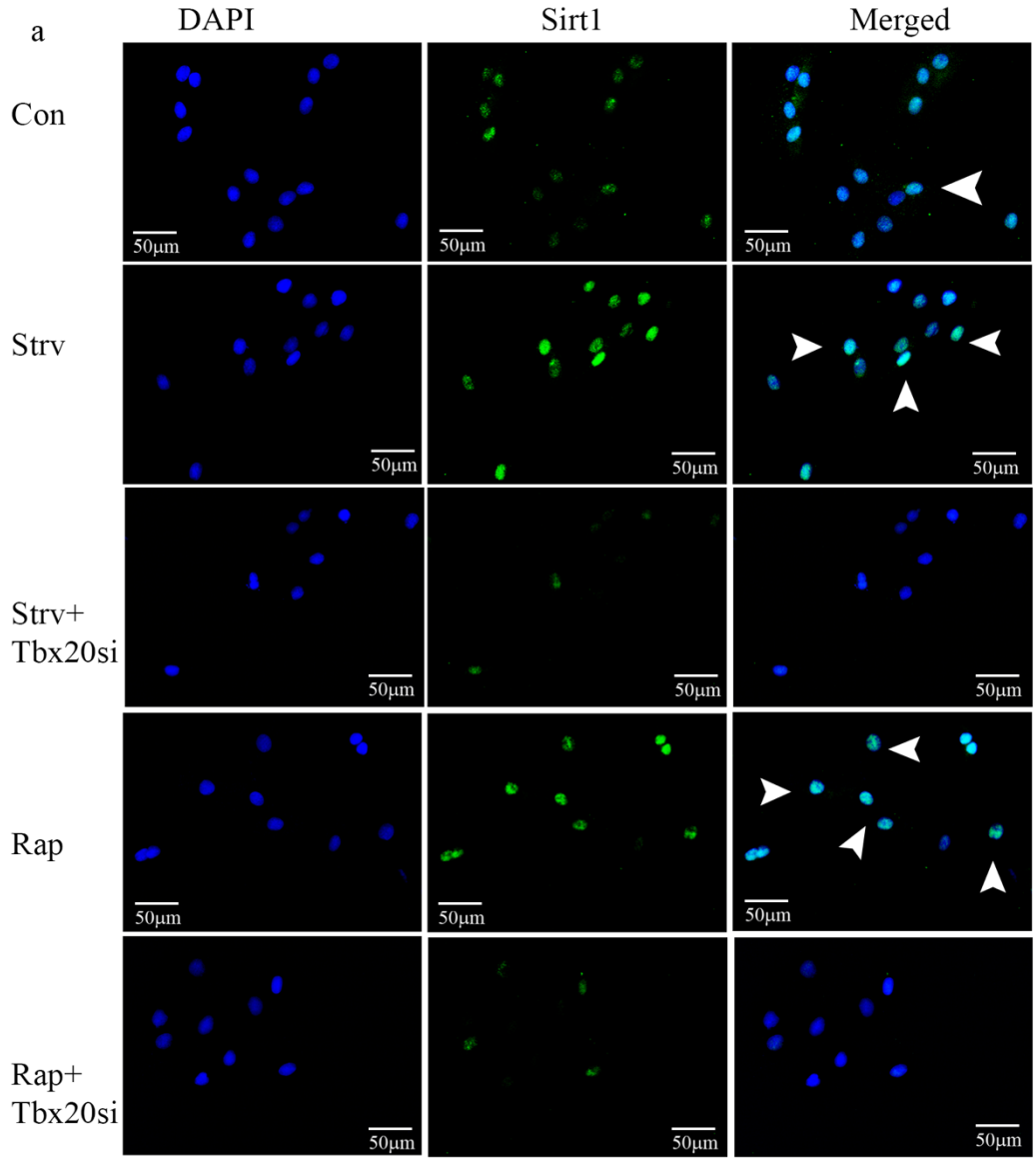
a
DAPI
Sirt1
Merged
Con
Strv
Strv+
Tbx20si
Rap
Rap+
Tbx20si
50μm

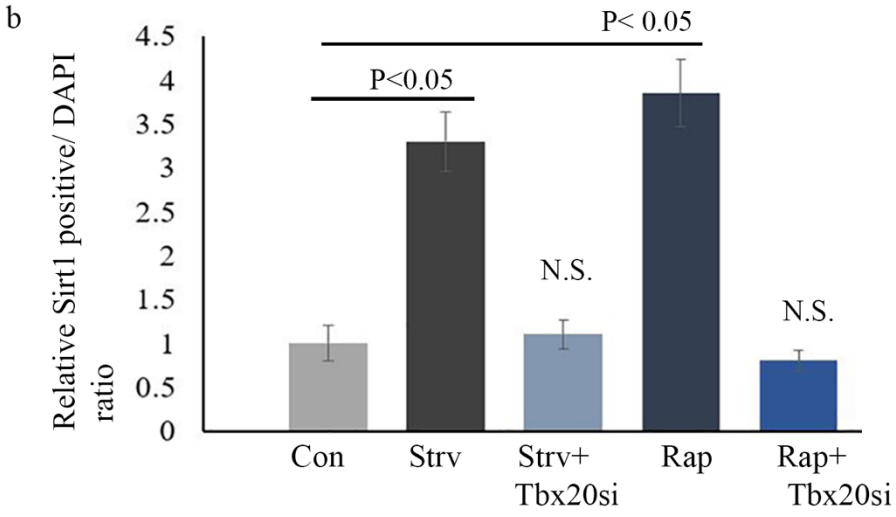
b
Relative Sirt1 positive/ DAPI ratio
4.5
4
3.5
3
2.5
2
1.5
1
0.5
0
P< 0.05
P<0.05
N.S.
N.S.
Con
Strv
Strv+
Tbx20si
Rap
Rap+
Tbx20si

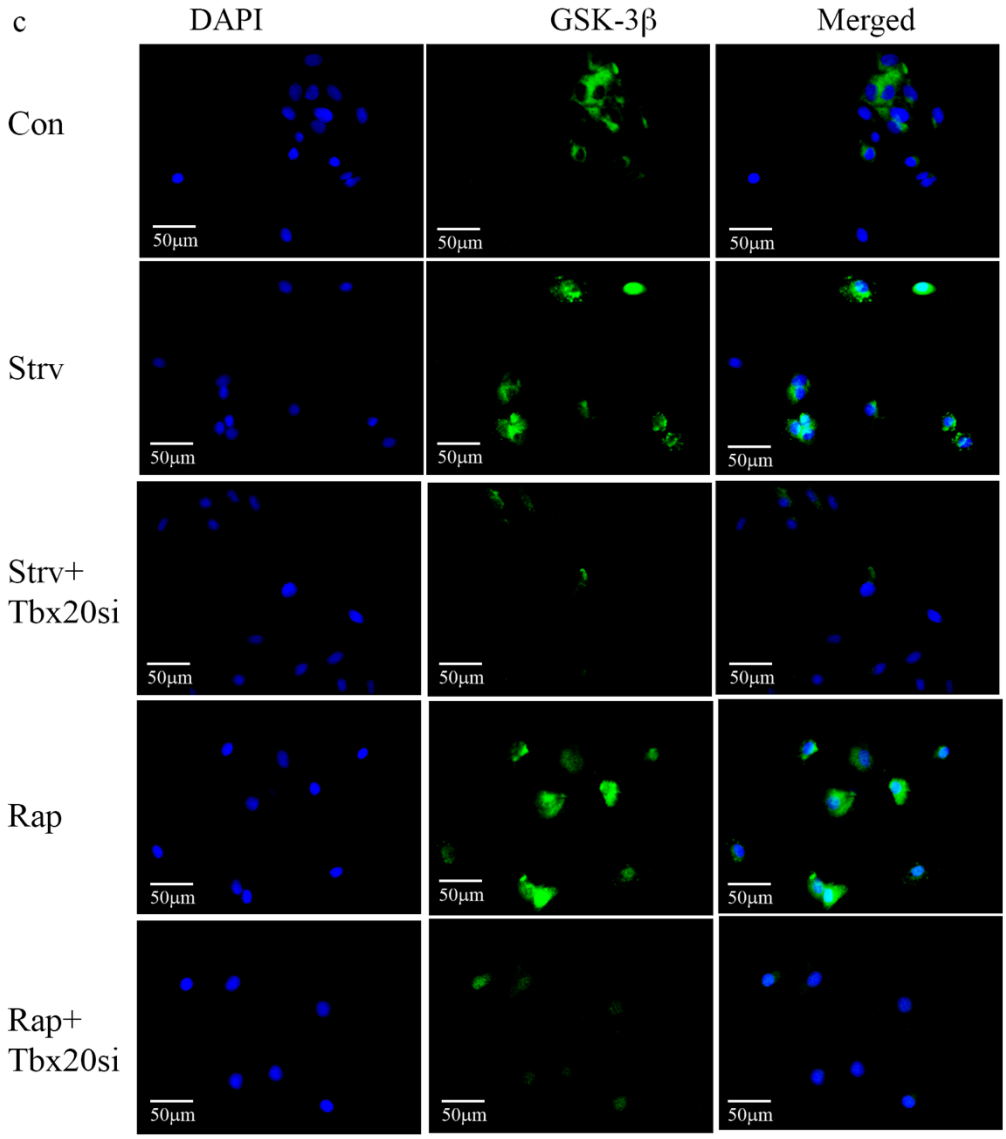
c
DAPI
GSK-3β
Merged
Con
Strv
Strv+
Tbx20si
Rap
Rap+
Tbx20si
50μm

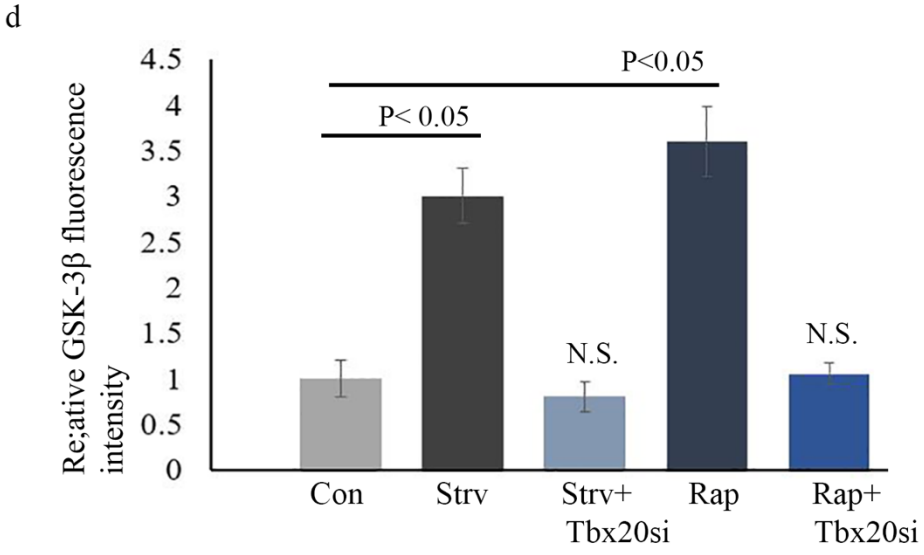
d
Re;ative GSK-3β fluorescence intensity
4.5
4
3.5
3
2.5
2
1.5
1
0.5
0
P<0.05
P< 0.05
N.S.
N.S.
Con
Strv
Strv+
Tbx20si
Rap
Rap+
Tbx20si

[*Figure 12: Tbx20 mediated regulation of Sirt1 and GSK-3β under autophagic conditions.* *Staining with anti-Sirt1 and anti-GSK3β antibodies (both shown in green) (Fig a and c) show a Tbx20 dependent expression pattern for both Sirt1 and GSK3β. The 3.2- and 3.7-fold increase in the relative no of Sirt1 positive cells for Strv and Rap treated H9c2 cells significantly reduced to 1.2 and 0.8-fold for Strv+Tbx20si and Rap+Tbx20si groups respectively (Fig. a, b). Similarly, the relative fluorescence intensity of GSK3β positive cells reduced to 0.8 and 0.9-fold for Strv+Tbx20si and Rap+Tbx20si cells from 3 and 3.5-fold observed for Strv and Rap treated cells (Fig. c, d). DAPI was used as nuclear stain (shown in blue). n=3, data analysed and expressed as mean ± SEM. Differences were considered statistically significant for $p < 0.05$.*]

D. Discussion

Impaired and low autophagy levels have been implicated in an array of pathological diseases including those related to age. High levels of ROS, low levels of antioxidants, low levels of NAD^+, poor mitochondrial integrity and mismanaged protein aggregates topped with underperforming autophagy machinery lead to clinical pathophysiology and these are hallmarks of an aging system.[119,120] The salient finding of this study is identifying the dual regulatory function of cardiac transcription factor Tbx20 under the influence of autophagy to restore and promote cardiac homeostasis, especially in the aging heart. Tbx20 being a transcription factor with a DNA binding site that has an affinity to T/2 site can interact with other transcription factors and proteins through its binding domain thereafter modulating the expression of its binding partners.[78,121,122] Known amongst other interacting partners of Tbx20 are Nkx2.5 and Gata4,[7] two other transcription factors important to cardiogenesis and markers of cardiac progenitors. It is a known fact that the efficiency of autophagy declines with age in general and in the heart also organ wise. The impaired autophagy machinery

in the aging heart leads to compromised cardiac integrity both structurally and physiologically.[19] Moreover, activation of autophagy is beneficial in reducing age related pathologies and improves senescence.[18,123,124] Here, we show the reactivation of Tbx20 after autophagic induction by two modes: starvation (nutrient stress) and rapamycin treatment in both the H9c2 cell line and aged murine model (Fig. 1,2 and 6). A characterised function of Tbx20 is proliferation but in our case, the elevated expression of Tbx20 did not help with cellular proliferation at all, in fact, it was on the contrary side with a slight decline observed in the proliferation rate compared to the control H9c2 cells (Fig. 3). Further, cell viability and apoptosis index measurement again showed a decline in the number of viable cells in the treated group and a slight increase in the apoptotic group, marked by a slightly enhanced expression of AG was again observed in the treated group (Fig. 4). This intrigued us to investigate what other role the upregulated expression of Tbx20 might play in this scenario. To solve this mystery, a bioinformatic tool was utilised and with the pre-existing knowledge of Tbx20's binding affinity to the sequence 5'-AGGTGT/CG/TA-3' and from the literature it is known that Sirt1 is a known anti-senescence marker beside the fact that it is activated under caloric restriction / intermittent fasting conditions. Not only that, studies show that AMPK inhibition attenuates the beneficial effects of Sirt1. The relationship between autophagy and Sirt11 is bidirectional, forming a positive feedback loop. Autophagy maintains cellular NAD+ levels, which are required for Sirt1 activity. Conversely, Sirt1 activation enhances autophagy by deacetylating key autophagy regulators. The reciprocal regulation of autophagy and Sirt11 ensures cellular homeostasis and adaptive responses to stress conditions. The decline in autophagy and SIRT1 activity is associated with aging and age-related diseases. Similarly, GSK-3β is a known regulator of cell growth and is a nutrient sensor. GSK3B is a multifunctional kinase involved in various cellular processes, including cell survival, proliferation, differentiation, and metabolism. It exists in two isoforms, GSK-3α

and GSK-3β, with GSK3β being the predominant isoform in the heart. GSK-3β activity is tightly regulated by phosphorylation at specific serine and tyrosine residues. When GSK3B is phosphorylated at serine 9, it becomes inactive and unable to phosphorylate its downstream targets. Moreover, GSK-3β regulates autophagy by phosphorylating ULK-1.[125] Interestingly, GSK-3β levels have been also found to decline with age and so is the cardioprotective role it offers.[114,115] Loss of GSK-3β has been linked with poor liver proliferation in aged mice while supplementing the same in aged mice improves proliferation.[126] While also, aged mice heterozygous for GSK-3β have been shown to lack both short and long term memory depicting the role of GSK-3β in memory retention in old age.[127] Moreover, Ser9 phosphorylated GSK-3β is pre-dominant in aging murine hearts suggesting a decline in the expression of GSK-3β. This poor level of GSK-3β suppresses autophagy in heart.[128] To our surprise, a perfect T/2 binding site was found in the promoter region of Sirt1 *Rattus norvegicus* and *Mus musculus* DNA sequence (Fig. 5) helping our case to move forward. Taking a cue from the in-silico data, the expression of Sirt1 along with GSK-3β, Nkx2.5 and Gata4 was assessed in the in-vivo scenario: the aged model mice subjected to starvation and rapamycin treatment and as anticipated the expression of Sirt1 and GSK-3β besides Tbx20 (Fig.7,8 and 9) both increased in the treatment group vs the aged control group. So was the expression of Nkx2.5 and Gata4 further re-affirming the already established regulatory role of Tbx20 in the expression of Nkx2.5 and Gata4,[3,102]To validate the Tbx20 dependent function of Gata4, Nkx2.5, Sirt1 and GSK-3β, H9c2 cell line was again relied on. Tbx20 siRNA mediated LOF assay was performed, the success of knockdown was verified by both immunostaining and WB (Fig. 10) and after knockdown, the expression of the 4 mentioned target proteins was assessed. As anticipated, Nkx2.5 and Gata4 both showed a marked decline in expression in groups with Tbx20si+Strv and Tbx20si+Rap treatment (Fig. 11) from only treatment groups. Much to our

surprise, Sirt1 and GSK-3β also followed quite a similar trend i.e., from the elevated expression observed in only treatment groups, there was a sharp decline in both Tbx20si+Strv and Tbx20si+Rap treatment groups (Fig. 12). This finding indicates a Tbx20 mediated functioning of both Sirt1 and GSK-3β in addition to that of Nkx2.5 and Gata4. Overall, Tbx20 works to improve cardiac homeostasis by promoting cardiomyocyte progenitor pool mediated through Nkx2.5 and Gata4 and on the other hand Tbx20 delays senescence in the heart by modulating the expression of GSK-3β and especially Sirt1.

Our findings, for the first time, proposes a two-way regulatory role of Tbx20 to promote cardiac homeostasis and improve cardiac aging under the influence of autophagy. In one direction the autophagy induced elevated Tbx20 interacts with and promotes the generation of cardiac progenitor like pool by inducing cardiac transcription factors Nkx2.5 and Gata4.[8,59,129] On the other hand, it induces the expression of Sirt1 and GSK-3β. The interaction between Tbx20 and Sirt1 is also reported for the first time in this study. The latter two genes especially Sirt1 is a well-known longevity promoter.[19,22,130] Sirt1 also has been implicated in its cardioprotective role. [21,23] Also, low levels of active GSK-3β and higher levels of pGSK-3β contribute to aging in the heart.[115] Impaired autophagy with age leads to a cellular catastrophe and while autophagy induction either through caloric restriction or by rapamycin treatment, senescence-related effects could be improved,[18,131] our work highlights a key underlying unexplored role played by Tbx20 in this scenario to provide cardio protection and improve cardiac aging by upregulating anti-senescence markers. This could lead to a futuristic approach to treating cardiac aging through the targeted expression of Tbx20.